**Table 1.** List of positive BACs in BAMCA analysis and summary of screening of candidate methylated genes (Cont'd)

| BAMCA ratio[†] | | mRNA expression | | | | Methylation[‡] | |
|---|---|---|---|---|---|---|---|
| GOTO | IMR32 | Stage I | IMR32 | GOTO | GOTO (+5-aza-dCyd)[§] | Stage I | Stage IVa |
| 3.46 | 4.57 | − | + | + | | | |
| 1.91 | 10.78 | | | | | | |
| 1.68 | 2.10 | + | − | − | + | − | + |
| | | + | + | + | | | |
| | | + | + | + | | | |
| 3.01 | 5.19 | + | + | + | | | |
| 2.10 | 2.05 | + | + | + | | | |
| 1.72 | 2.33 | + | + | + | | | |
| 3.07 | 5.54 | + | + | + | | | |
| 2.54 | 2.32 | + | + | | | | |
| | | + | + | + | | | |
| 3.52 | 2.17 | + | − | + | | | |
| 3.31 | 2.48 | + | − | − | − | | |
| 3.89 | 5.45 | + | + | + | | | |
| 3.72 | 12.90 | + | − | + | | | |
| 2.06 | 1.45 | + | + | + | | | |
| 2.51 | 3.51 | − | − | − | | | |
| | | + | + | + | | | |
| | | + | + | − | | | |
| 1.81 | 1.85 | + | + | + | | | |
| | | + | + | + | | | |
| 1.75 | 16.90 | + | − | − | − | | |
| | | + | − | − | ± | − | ± |
| 2.93 | 3.24 | + | − | − | + | − | ± |
| | | + | − | − | + | − | ± |
| 1.54 | 3.39 | + | + | + | | | |
| | | − | + | + | | | |

**Methylation of *NR1I2* CpG island in neuroblastoma cell lines.** We next examined the methylation status of the slightly CpG-rich 5′ region (region 1) and the CpG island including exon 3 (region 2) of the *NR1I2* gene, which had been detected by the National Center for Biotechnology Information (NCBI) human genome database[6] as shown in Fig. 1*E*. Bisulfite sequencing analysis of region 2 revealed aberrant DNA hypermethylation in IMR32 and SH-SY5Y cell lines lacking expression of *NR1I2*, but hypomethylation in two lines expressing the gene (SK-N-AS and SK-N-KP) and in a normal lymphoblast cell line (LCL). On the other hand, no significant difference in methylation pattern within region 1 was observed among those four neuroblastoma cell lines and LCL, regardless of expression status. We did COBRA to confirm the relationship between expression and methylation status within region 2 in a larger set of neuroblastoma cell lines. Predominant methylated alleles were detected in all lines lacking *NR1I2* expression (Fig. 1*F* and data not shown).

Because several splicing variants of *NR1I2*, including the variant starting transcription from exon 3 (variant 4, v4), have been reported in various human tissues (19),[7] we did RT-PCR using specific primers for each variant to examine which transcripts might be silenced through a DNA methylation within region 2 in neuroblastoma cell lines (Fig. 1*G*). Variant 1, the most major variant in various human tissues, and variant 2 were expressed in unmethylated neuroblastoma cell lines, but not in methylated lines, whereas variant 4 without open reading frame was not expressed in one of the unmethylated cell lines (SK-N-AS). The expression of variant 1 and variant 4 was restored after the treatment with 5-aza-dCyd in methylated neuroblastoma cell lines, whereas the expression of variant 2 was not. Variant 3, lacking a part of exon 5, was not expressed in neuroblastoma cell lines regardless of methylation status within CpG island and 5-aza-dCyd treatment. Those results suggested that the methylation of CpG residues in region 2 might be mainly responsible for the silencing of variant 1 of the *NR1I2* gene starting transcription from exon 1a in neuroblastoma, although region 2 does not contain its transcriptional start site.

**Promoter activity of the CpG island located around exon 3 of *NR1I2*.** Because the CpG island (region 2) of *NR1I2* was located around exon 3, we first determined whether region 2 had promoter activity by means of a luciferase reporter assay. This fragment alone (Fig. 2*A*, *2/L*) revealed clear promoter activity, whereas region 1 fragment upstream of exon 1 (Fig. 2*A*, *1/L*) showed almost none (Fig. 2*B*). In addition, we next determined whether region 2 acts as an enhancer to stimulate transcription from exon 1 by testing the luciferase activity in construct

[6] http://www.ncbi.nlm.nih.gov/.
[7] http://www.ncbi.nlm.nih.gov/IEB/Research/Acembly/index.html.

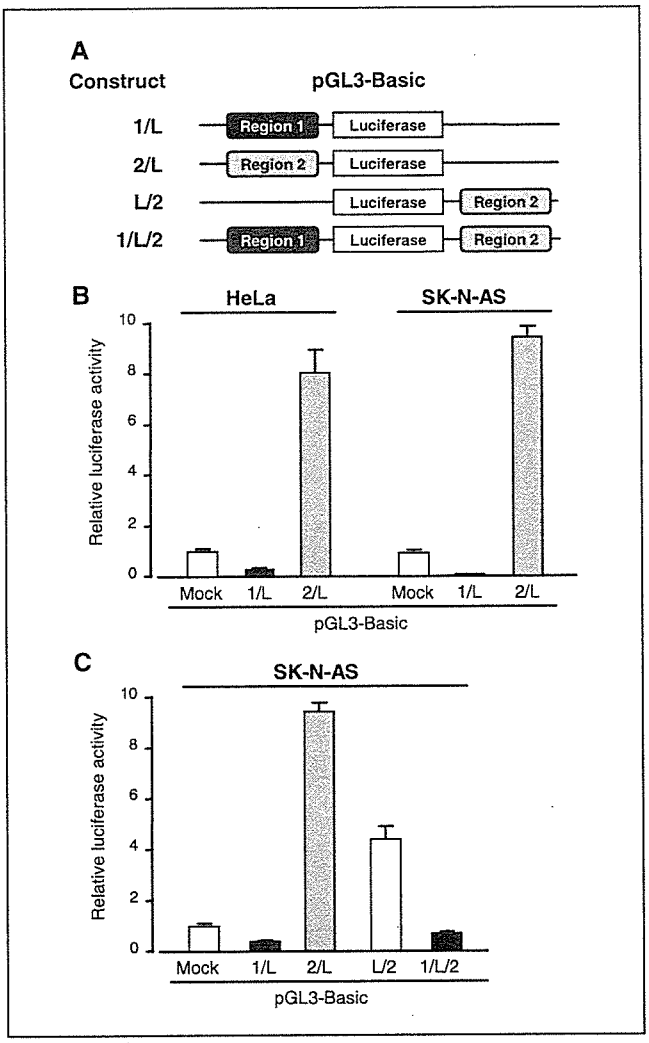


**Figure 2.** Promoter activity of the CpG island of *NR1I2*. pGL3-Basic vector, each containing a 1,060 bp 5′ fragment (region 1) or a 480 bp CpG island (region 2) of *NR1I2* in front of and/or downstream of the luciferase gene (*1/L*, *2/L*, *L/2*, and *1/L/2*; *A*), or pGL3-Basic empty vector (mock), was transfected into HeLa or SK-N-AS cells to evaluate promoter activity of region 1 and region 2 (*B*) and enhancer activity of region 2 (*C*). Luciferase activities were normalized versus an internal control. *Columns*, means of three separate experiments, each done in triplicate; *bars*, SE.

containing region 1 in front of the luciferase reporter gene and region 2 downstream of the luciferase gene (Fig. 2*A*, *1/L/2*). Although region 2 downstream of the luciferase gene (Fig. 2*A*, *L/2*) showed some promoter activity, region 2 revealed no enhancer activity for region 1 (Fig. 2*C*).

**Analysis of *NR1I2* methylation and expression in primary neuroblastoma tumors.** We next examined methylation status of the *NR1I2* CpG island in 51 surgically resected primary neuroblastomas using COBRA (Table 2). Clearly methylated alleles were detected in nine of the tumors (17%; Fig. 3*A*). The appearance of partial methylation observed in those nine tumors can be explained by the unavoidable contamination of nontumorous cells in the specimens. Five of the nine tumors (55%) had undergone *MYCN* amplification, whereas only 3 of 42 (7%) unmethylated tumors showed amplification of *MYCN* (Table 2). Moreover, methylation of region 2 of the *NR1I2* gene was more frequently detected in advanced tumors (stages III and IVa; $P$ = 0.0234, Fisher's exact test), tumors from patients with poor outcome (dead from disease; $P$ = 0.0135, Fisher's exact test), and tumors from patients >1 year old ($P$ = 0.052, Fisher's exact test), although the difference did not quite reach statistical significance in terms of patient age. In the 47 neuroblastoma cases where high-quality RNAs were available for expression analysis, a clear correlation between the methylation status of the CpG island and expression level of *NR1I2* mRNA was observed (Fig. 3*B* and *C*). By means of real-time quantitative RT-PCR experiments, we saw a statistically significant inverse correlation between expression of *NR1I2* mRNA and tumor stage ($P$ = 0.0137, Mann-Whitney $U$ test) or *MYCN* amplification ($P$ = 0.0003, Mann-Whitney $U$ test; Fig. 3*C*).

**Suppression of cell growth after restoration of NR1I2 expression.** To gain further insight into the potential role of NR1I2 in neuroblastoma carcinogenesis, we investigated whether restoration of NR1I2 expression would suppress growth of neuroblastoma cells lacking endogenous *NR1I2* expression using two *NR1I2* expression constructs, a Myc-tagged full coding sequence of *NR1I2* alone (pCMV-Tag3-*NR1I2*) and one fused to the constitutively active herpes virus VP-16 transactivation domain (pCMV-Tag3-*VP-NR1I2*). The VP-16-NR1I2 chimeric protein showed stronger transactivating activity than NR1I2 alone in a reporter assay using a reporter construct containing *NR1I2* response elements from the *CYP3A4* promoter (data not shown). After selecting drug-resistant colonies in transient transfection experiments, we found that colonies of *NR1I2*-transfected cells were remarkably fewer than in cultures of control transfectants and the effect of VP-16-NR1I2 was much greater than that of NR1I2 (Fig. 4*A*). Furthermore, VP-16-NR1I2 stable transfectants

**Table 2.** Correlation between patient profiles and *NR1I2* methylation status in 51 cases with neuroblastoma

| Characteristics | Cases *n* | COBRA on *NR1I2* region 2* | | |
|---|---|---|---|---|
| | | Negative *n* | Positive *n* | *P*† |
| Total | 51 | 42 | 9 | |
| Age (y) | | | | |
| <1 | 33 | 30 | 3 | 0.052 |
| ≥1 | 18 | 12 | 6 | |
| Stage‡ | | | | |
| I, II, IVS | 30 | 23 | 2 | **0.0234** |
| III, IVa | 21 | 16 | 7 | |
| *MYCN* | | | | |
| Nonamplified | 43 | 39 | 4 | **0.024** |
| Amplified | 8 | 3 | 5 | |
| Outcome | | | | |
| Alive | 44 | 39 | 5 | **0.0135** |
| Dead | 7 | 3 | 4 | |

NOTE: Statistically significant values are in boldface.
*COBRA was done as described in Materials and Methods.
†*P* values are from Fisher's exact test and were statistically significant when <0.05.
‡Tumor stage was classified according to the International Neuroblastoma Staging System.

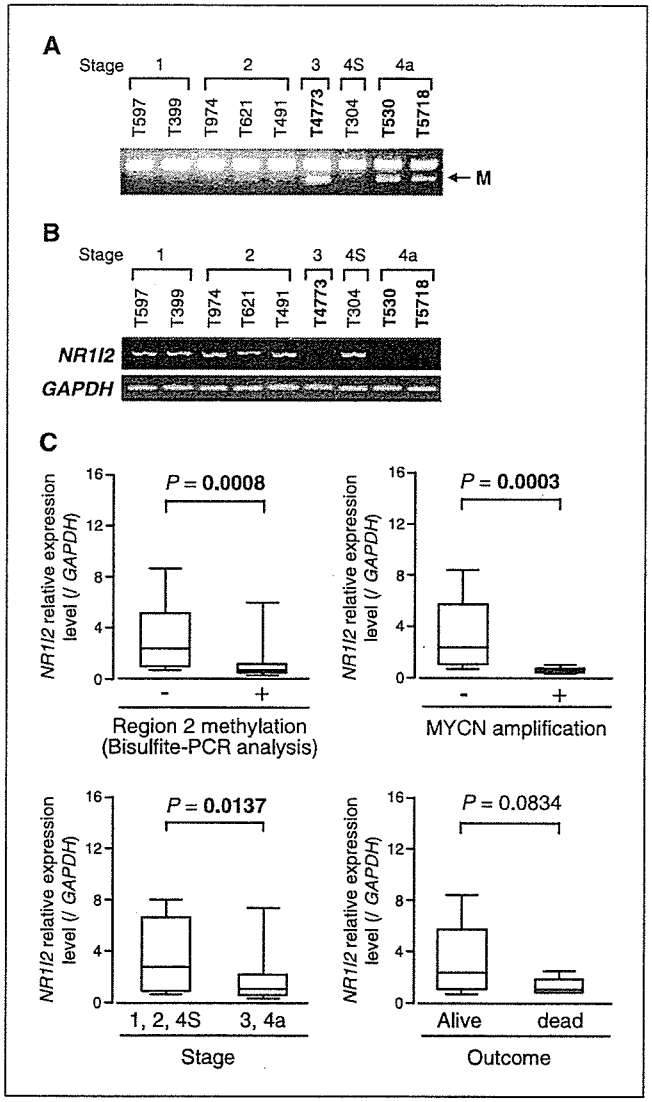


**Figure 3.** Methylation status and expression levels of *NR1I2* in primary neuroblastoma tumors. *A*, representative results of COBRA of the *NR1I2* CpG island (region 2). *M*, methylated alleles restricted by *Hha*I. *B*, representative results of RT-PCR analysis of *NR1I2* mRNA expression. *GAPDH* was used as an internal control. Note that tumors showing methylation in Fig. 2*A* (T4773, T530, and T5718) showed decreased expression of *NR1I2*. *C*, expression of *NR1I2* mRNA in primary neuroblastoma tumors, compared with methylation status of the CpG island of *NR1I2* region 2, *MYCN* amplification status, tumor stage, and patient outcomes. The levels of *NR1I2* mRNA expression were determined by real-time quantitative RT-PCR experiments. Significantly higher expression of *NR1I2* was observed in tumors without methylation of the CpG island ($P = 0.0008$; Mann-Whitney *U* test), in stage I, II, and IVS tumors ($P = 0.0137$, Mann-Whitney *U* test), and in *MYCN*-nonamplified tumors ($P = 0.0003$, Mann-Whitney *U* test) compared with tumors with methylation of the CpG island, stage III or IVa tumors, and *MYCN*-amplified tumors. Higher expression of *NR1I2* was also observed in living, disease-free patients compared with those who had died of their tumors, although the difference did not reach statistical significance ($P = 0.0834$, Mann-Whitney *U* test).

established from a cell line (SMS-KAN) without endogenous expression of this gene showed a lower growth rate than control vector-transfected cells regardless of VP-16-NR1I2 expression level (Fig. 4*B* and *C*). The same result was obtained in other cell line (data not shown).

**Screening of possible target genes for NR1I2.** To identify possible transcriptional targets for NR1I2, we did expression array analysis in an independent VP-16-NR1I2 stable transfectant established from SMS-KAN, in a comparison with vector-transfected cells. We twice obtained independent experimental data (first, Cy3-B1/Cy5-vector; second, Cy5-B1/Cy3-vector) and compiled a list of 105 genes that showed ratios >1.5 in both experiments (Supplementary Table S1). Semiquantitative RT-PCR analysis revealed up-regulation of *CYP3A4*, a known transcriptional target of *NR1I2*, in VP-16-NR1I2 stable transfectant, indicating the reliability of our system for detecting target genes (Supplementary Fig. S1). To validate the expression array data, we did semiquantitative RT-PCR analyses of 10 other genes (Fig. 4*D*), which have been previously reported as tumor-associated genes, using two independent VP-16-NR1I2 stable transfectants established from SMS-KAN cells (KAN-B1 and KAN-B2) and one stable transfectant from GOTO cells (GOTO-A1). GOTO-A1 also showed a lower growth rate than control vector-transfected cells (data not shown). The RT-PCR results for KAN-B1 confirmed up-regulation of seven genes except for *BARD1*, *EXT1*, and *MCM5* (Fig. 4*D*). Notably, only *PLA2G2A* showed increased expression in all stable transfectants examined compared with their control cells (Fig. 4*D*; Supplementary Fig. S1).

## Discussion

In the study presented here, we identified a novel target for CpG island methylation, *NR1I2*, observed mainly in advanced neuroblastomas, through a genome-wide exploration of highly methylated DNA fragments using BAMCA. A clear inverse correlation emerged between CpG island methylation and the expression status of *NR1I2* both in cell lines and primary tumors of neuroblastoma (i.e., hypermethylation and silencing of *NR1I2* were more frequent in advanced neuroblastoma tumors). Together with a shown growth suppressive effect of exogenous NR1I2, the data suggested that *NR1I2* was likely to be a tumor suppressor gene associated with clinical and/or biological aggressiveness of neuroblastoma. Our results further underscored the promise of BAMCA as a high-throughput screening method for methylated sites in cancer genomes on an array platform.

BAMCA, however, has some disadvantages: (*a*) It examines only a limited number of CpG sites within a CpG island because only *Sma*I/*Xma*I sites are used to search differentially methylated CpGs. (*b*) It identifies BACs, which contain differentially methylated sequences between test and reference DNAs, although sequences are not always associated with promoter regions of genes. (*c*) It misses differentially methylated sequences/genes without BACs spotted on the BAC array used. To improve the sensitivity of array-based methylation screening, it is possible to use other methylation-sensitive restriction sites as indicators, including *Not*I site (20). However, BAMCA may quickly provide the list of possible target genes for methylation within identified BAC clones using information from human genome database without cloning and sequencing of enriched fragments, suggesting that it may have important applications in population-based studies of CpG island methylation.

*NR1I2* locates at 3q13.33, a chromosomal region that is not often involved in loss of heterozygosity or copy number losses in neuroblastoma (21, 22). Indeed, most of the cell lines we used in this study showed normal copy number in 3q (13), suggesting that a homozygous inactivation of *NR1I2* might occur by biallelic

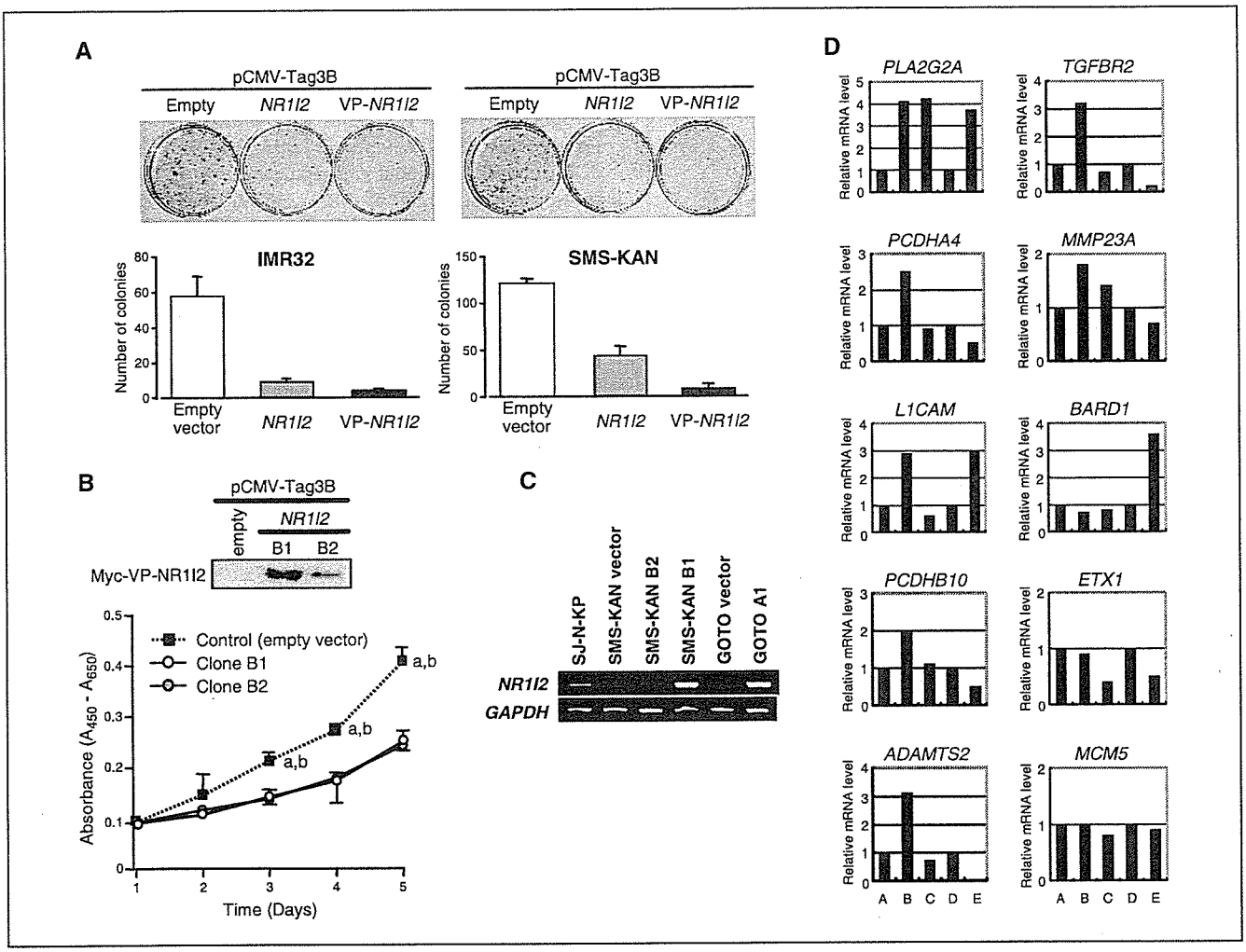


**Figure 4.** Effect of restoration of NR1I2 expression on growth of neuroblastoma cells. *A, top,* colony formation assays using neuroblastoma cell lines. Cells without *NR1I2* expression (IMR32 and SMS-KAN) were transfected with Myc-tagged construct containing *NR1I2* (pCMV-Tag3B-*NR1I2*), *VP-NR1I2* (pCMV-Tag3B-*VP-NR1I2*), or empty vector (pCMV-Tag3B), and selected for 3 weeks with G418. *Bottom,* quantitative analysis. *Columns,* mean of three separate experiments, each done in triplicate; *bars,* SE. *B,* inhibitory effect of stably transfected *NR1I2* on the growth of SMS-KAN cells transfected with pCMV-Tag3B-*VP-NR1I2* or empty vector and selected with G418 to establish clones stably expressing NR1I2. *Top,* two clones transfected with pCMV-Tag3B-*VP-NR1I2* (B1 and B2) were subjected to Western blot analysis using 10 μg of protein extract and anti-Myc-Tag antibody. Both expressed Myc-tagged VP-NR1I2 protein. *Bottom,* effect of stable NR1I2 expression on the growth of SMS-KAN cells. Cell viability was determined by water-soluble tetrazolium salt assay at the indicated times. *Points,* means of three separate experiments; *bars,* SE. Statistical analysis used the Mann-Whitney *U* test: *a,* control versus clone B1; *b,* control versus clone B2. All $P < 0.05$. *C,* the mRNA expression level of *NR1I2* in endogenously NR1I2-positive cells (SK-N-KP) as well as stably transfected cells (SMS-KAN-B1, SMS-KAN-B2, and GOTO-A1) and their mock-transfected control (KAN-vector and GOTO-vector). *D,* confirmation of microarray results by semiquantitative RT-PCR of possible target genes using two stable transfectants established from SMS-KAN (KAN-B1 and KAN-B2) and one transfectant from GOTO (GOTO-A1) with their mock-transfected control cells *A,* SMS-KAN mock-control; *B,* KAN-B1; *C,* KAN-B2; *D,* GOTO mock-control; *E,* GOTO-A1. PCR products were electrophoresed in 3% agarose gel and band quantification was done with LAS-3000 (Fujifilm, Tokyo, Japan). After normalization with *GAPDH*, expression level of each gene in each transfectant relative to its corresponding mock-transfected control was recorded as a fold increase in relative expression level. Primer sequences and cycling numbers for PCR of each gene are available on request.

methylation. Similar findings have been reported for several genes, such as *RASSF1* (3p21.3), *DAPK* (9q34.1), and *THBS1* (15q15), which are located in regions not frequently deleted, although some methylated genes, such as *ARF* and *INK4A* (9p21), and *CASP8* (2q23), are in fact on regions frequently deleted in neuroblastoma (23). Therefore, both biallelic methylation and monoallelic methylation with allele loss may be important mechanisms for inactivating tumor-associated genes in this disease.

Our promoter assays showed that CpG island around exon 3 (region 2) shows promoter activity, but CpG-rich 5′ region containing exon 1 and its 5′ upstream sequences (region 1) does not. Region 2 shows no enhancer activity for region 1 (Fig. 2). The methylation status of region 2, but not region 1, was highly and inversely correlated with the expression of *NR1I2*, especially the most major variant of *NR1I2*, variant 1, starting from exon 1a. Those results suggest that the methylation status of CpG residues in region 2 might be responsible for the silencing of this gene and contributed to loss of function of NR1I2 protein in neuroblastoma. A few studies, including ours, have shown that promoter activity can occur in fragments, especially CpG islands, not containing transcriptional starting sites (17, 24, 25). It is possible that methylation that occurred in those CpG islands with promoter activity may silence gene expression from specific starting sites.

Among numerous hypermethylated genes reported in neuroblastoma (3–8), *CASP8* seems to be inactivated through promoter methylation in advanced neuroblastoma tumors where *MYCN* is amplified (4). Those findings, along with ours, suggest that (*a*) unknown mechanisms contribute to progression of neuroblastoma by causing genetic alterations, including *MYCN* amplification, as well as methylation-mediated inactivation of a subset of tumor suppressor genes; (*b*) methylation-mediated inactivation of a subset of tumor suppressor genes may cause genetic changes that lead to progression of neuroblastoma; or (*c*) *MYCN* amplification and/or other alterations in advanced neuroblastomas may bring about a CpG island methylator phenotype (3). Gonzalez-Gomez et al. (23) reported that higher aggressiveness, represented at the molecular level by concurrent *MYCN* amplification and 1p loss in neuroblastoma, was not paralleled by an accumulation of methylation events among various genes they examined, suggesting that CpG island methylation in advanced neuroblastoma could be specific to a subset of genes.

The *NR1I2* gene encodes an orphan nuclear receptor that plays a key role in the regulation of xenobiotic response by controlling expression of drug metabolizing and clearance molecules (26–28). NR1I2 protein activates expression of genes encoding proteins such as CYP3A4 and ABCB1, which reduce the concentrations of xenochemicals and toxic bile acids (29). However, effects of NR1I2 on cell growth or expression of growth-regulating genes have never been clarified, although we have shown here that the induction of ectopic NR1I2 inhibited growth of neuroblastoma cells. Other nonsteroidal nuclear receptors, such as all-*trans* retinoic acid receptor and vitamin $D_3$ receptor, which form heterodimers with the 9-*cis* retinoic acid receptor in the same way as NR1I2, mediate antiproliferative and differentiation-promoting activities toward several malignant cell types (30, 31). Therefore, growth-suppressive activity might be one of the normal functions of NR1I2 although its mechanisms remain unknown.

To achieve some clarity with respect to the growth inhibitory activity of NR1I2, we tried to determine its putative transcriptional targets. Among 105 genes through an expression array analysis, we selected 10 genes for validation by semiquantitative PCR based on their possible cancer-associated function (Online Mendelian Inheritance in Man),[8] and identified one candidate, *PLA2G2A*, encodes secretory phospholipase A2, as a possible target of NR1I2, although it will be needed to determine whether *PLA2G2A* is a direct or indirect target. This product qualifies as a tumor suppressor because mice lacking *PLA2G2A* expression show increased colonic polyposis (32). Interestingly, *PLA2G2A* was mapped to chromosome 1p36, a region frequently implicated in the pathogenesis of neuroblastoma (33). Further screening of possible targets of NR1I2 will be necessary to clarify how NR1I2 regulates neuroblastoma cell growth.

Because only 7 of 51 neuroblastoma patients in our study died during follow-up periods, we did not perform a survival analysis. However, the high prevalence of *NR1I2* silencing through DNA methylation that we observed in aggressive neuroblastomas, along with the shown growth suppression activity of NR1I2, indicate that this molecule might serve as a diagnostic marker to predict prognosis.

## Acknowledgments

Received 3/30/2005; revised 9/2/2005; accepted 9/13/2005.

**Grant support:** Grants-in-Aid for Scientific Research on Priority Areas (C) from the Ministry of Education, Culture, Sports, Science, and Technology, Japan; a Grant-in-Aid from Core Research for Evolutionary Science and Technology of Japan Science and Technology; Center of Excellence program for Frontier Research on Molecular Destruction and Reconstitution of Tooth and Bone; program for promotion of Fundamental Studies in Health Sciences of the Pharmaceuticals and Medical Devices Agency; and Third Term Comprehensive Control Research for Cancer of the Ministry of Health, Labour, and Welfare.

The costs of publication of this article were defrayed in part by the payment of page charges. This article must therefore be hereby marked *advertisement* in accordance with 18 U.S.C. Section 1734 solely to indicate this fact.

We thank Ai Watanabe and Ayako Takahashi for technical assistance.

[8] http://www.ncbi.nlm.nih.gov/Omim/omimhelp.html.

## References

1. Brodeur GM. Neuroblastoma: biological insights into a clinical enigma. Nat Rev Cancer 2003;3:203–16.
2. Westermann F, Schwab M. Genetic parameters of neuroblastomas. Cancer Lett 2002;184:127–47.
3. Abe M, Ohira M, Kaneda A, et al. CpG island methylator phenotype is a strong determinant of poor prognosis in neuroblastomas. Cancer Res 2005;65:828–34.
4. Teitz T, Wei T, Valentine MB, et al. Caspase 8 is deleted or silenced preferentially in childhood neuroblastomas with amplification of MYCN. Nat Med 2000;6:529–35.
5. Astuti D, Agathanggelou A, Honorio S, et al. RASSF1A promoter region CpG island hypermethylation in phaeochromocytomas and neuroblastoma tumours. Oncogene 2001;20:7573–7.
6. Yan P, Muhlethaler A, Bourloud KB, Beck MN, Gross N. Hypermethylation-mediated regulation of CD44 gene expression in human neuroblastoma. Genes Chromosomes Cancer 2003;36:129–38.
7. Yang Q, Liu S, Tian Y, et al. Methylation-associated silencing of the thrombospondin-1 gene in human neuroblastoma. Cancer Res 2003;63:6299–310.
8. Yang Q, Liu S, Tian Y, et al. Methylation-associated silencing of the heat shock protein 47 gene in human neuroblastoma. Cancer Res 2004;64:4531–8.
9. Baylin SB, Herman JG, Graff JR, Vertino PM, Issa JP. Alterations in DNA methylation: a fundamental aspect of neoplasia. Adv Cancer Res 1998;72:141–96.
10. Ushijima T. Detection and interpretation of altered methylation patterns in cancer cells. Nat Rev Cancer 2005;5:223–31.
11. Toyota M, Ho C, Ahuja N, et al. Identification of differentially methylated sequences in colorectal cancer by methylated CpG island amplification. Cancer Res 1999;59:2307–12.
12. Inazawa J, Inoue J, Imoto I. Comparative genomic hybridization (CGH)-arrays pave the way for identification of novel cancer-related genes. Cancer Sci 2004;95:559–63.
13. Saito-Ohara F, Imoto I, Inoue J, et al. PPM1D is a potential target for 17q gain in neuroblastoma. Cancer Res 2003;63:1876–83.
14. Brodeur GM, Pritchard J, Berthold F, et al. Revision of the international criteria for neuroblastoma diagnosis, staging, and response to treatment. J Clin Oncol 1993;11:1466–77.
15. Matsumura T, Michon J. Treatment of localized neuroblastoma. In: Brodeur GM, Sawada T, Tsuchida Y, Voute PA, editors. Neuroblastoma. Amsterdam (the Netherlands): Elsevier Science BV; 2000. p. 403–16.
16. Tsuchida Y, Kaneko M. Treatment of advanced neuroblastoma: the Japanese experience. In: Brodeur GM, Sawada T, Tsuchida Y, Voute PA, editors. Neuroblastoma. Amsterdam (the Netherlands): Elsevier Science BV; 2000. p. 453–70.
17. Sonoda I, Imoto I, Inoue J, et al. Frequent silencing of low density lipoprotein receptor-related protein 1B (LRP1B) expression by genetic and epigenetic mechanisms in esophageal squamous cell carcinoma. Cancer Res 2004;64:3741–7.
18. Inoue J, Otsuki T, Hirasawa A, et al. Overexpression of PDZK1 within the 1q12-q22 amplicon is likely to be associated with drug-resistance phenotype in multiple myeloma. Am J Pathol 2004;165:71–81.
19. Lamba V, Yasuda K, Lamba JK, et. al. PXR (NR1I2): splice variants in human tissues, including brain, and identification of neurosteroids and nicotine as PXR activators. Toxicol Appl Pharmacol 2004;199:251–65.
20. Ching TT, Maunakea AK, Jun P, et al. Epigenome analyses using BAC microarrays identify evolutionary conservation of tissue-specific methylation of *SHANK3*. Nat Genet 2005;37:645–51.
21. Brinkschmidt C, Christiansen H, Terpe HJ, et al. Comparative genomic hybridization (CGH) analysis of neuroblastomas—an important methodological approach in paediatric tumour pathology. J Pathol 1997;181:394–400.
22. Takita J, Hayashi Y, Yokota J. Loss of heterozygosity in neuroblastomas—an overview. Eur J Cancer 1997;33:1971–3.
23. Gonzalez-Gomez P, Bello MJ, Lomas J, et al. Aberrant methylation of multiple genes in neuroblastic tumours. Relationship with MYCN amplification and allelic status at 1p. Eur J Cancer 2003;39:1478–85.
24. Kolb A. The first intron of the murine β-casein gene contains a functional promoter. Biochem Biophys Res Commun 2003;306:1099–105.

25. Nakagawachi T, Soejima H, Urano T, et al. Silencing effect of CpG island hypermethylation and histone modifications on *O6*-methylguanine-DNA methyltransferase (MGMT) gene expression in human cancer. Oncogene 2003;22:8835–44.
26. Blumberg B, Sabbagh W, Juguilon H, et al. SXR, a novel steroid and xenobiotic-sensing nuclear receptor. Genes Dev 1998;12:3195–205.
27. Kliewer SA, Moore JT, Wade L, et al. An orphan nuclear receptor activated by pregnanes defines a novel steroid signaling pathway. Cell 1998;92:73–82.
28. Xie W, Barwick JL, Downes M, et al. Humanized xenobiotic response in mice expressing nuclear receptor SXR. Nature 2000;406:435–9.
29. Synold TW, Dussault I, Forman BM. The orphan nuclear SXR coordinately regulates drug metabolism and efflux. Nat Med 2001;7:584–90.
30. Altucci L, Gronemeyer H. Nuclear receptors in cell life and death. Trends Endocrinol Metab 2001;12:460–8.
31. Rao A, Coan A, Welsh JE, Barclay WW, Koumenis C, Cramer SD. Vitamin D receptor and p21/WAF1 are targets of genistein and 1,25-dihydroxyvitamin $D_3$ in human prostate cancer cells. Cancer Res 2004;64:2143–7.
32. Haluska FG, Thiele C, Goldstein A, Tsao H, Benoit EP, Housman D. Lack of phospholipase A2 mutations in neuroblastoma, melanoma and colon-cancer cell lines. Int J Cancer 1997;72:337–9.
33. Praml C, Savelyeva L, Le Paslier D, et al. Human homologue of a candidate for the Moml locus, the secretory type II phospholipase A2 (PLA2S-II), maps to 1p35–36.1/D1S199. Cancer Res 1995;55:5504–6.

Available online at www.sciencedirect.com
SCIENCE DIRECT
Cancer Letters 228 (2005) 267–270
CANCER Letters
www.elsevier.com/locate/canlet

# Diversity in neuroblastomas and discrimination of the risk to progress

Takeo Tanaka[a,*], Tomoko Iehara[b], Tohru Sugimoto[b], Minoru Hamasaki[c], Satoshi Teramukai[d], Yoshiaki Tsuchida[e], Michio Kaneko[e], Tadashi Sawada[b,d]

[a]*Department of Pediatrics and Division of Clinical Research, National Hospital Organization, Kure Medical Center, Hiroshima, Japan*
[b]*Department of Pediatrics, Kyoto Prefectural University of Medicine, Kyoto, Japan*
[c]*Department of Pathology, Shizuoka Children's Hospital, Shizuoka, Japan*
[d]*The Japanese Infantile Neuroblastoma Cooperative Study*
[e]*The Japanese Advanced Neuroblastoma Cooperative Study*

Received 26 November 2004; accepted 2 December 2004

**Abstract**

The clinical diversity of Neuroblastomas (NBs) was discriminated into three groups with high sensitivity and specificity to patient's outcome. The '*high risk*' NB is defined with any of following conditions, MYCN amplification or unfavorable histology of International Neuroblastoma Pathological Classification (INPC) or low Ha-ras/trk A expression. The '*low risk*' NB is defined with all following conditions, single copy of MYCN and INPC favorable histology and high Ha-ras/trk A expression and localized tumor. The remaining NBs were classified into '*intermediate risk*' ones. According to these criteria, the diversity of the 248 mass-screening NBs was shown with variety progressive risk; 40% were classified in *low risk group*, 25% were in *high risk group* and 35% were in *intermediate risk group*.


*Keywords:* Neuroblastoma; Risk discrimination; *MYCN*; INPC; Ha-ras; Trk A; Mass-screening.

## 1. Introduction

Neuroblastoma (NB) is the most common extracranial solid malignancy in childhood. This malignancy shows diversity in their clinical behavior. Recent advances in molecular and genetic approach promote to understand their biology and provide predictors associated with clinical behavior of NBs [1]. MYCN amplification is a powerful predictor with high specificity to aggressiveness of NBs [2], however, the sensitivity is only a half of the patients with poor clinical outcome [3]. Brodeur [4] proposed three types of NBs classified according to several biological markers. The clinical evaluation whether we can get predictive specificity and sensitivity enough to use for the patients has not been done yet.

* Corresponding author. Tel.: +81 823 22 3111; fax: +81 823 22 0478.
*E-mail address:* ttanaka@kure-nh.go.jp (T. Tanaka).

0304-3835/$ - see front matter © 2005 Elsevier Ireland Ltd. All rights reserved.
doi:10.1016/j.canlet.2004.12.051

## 2. Ha-ras and trk A expression in NBs

We first reported that the Ha-ras expression associated closely with the clinical outcome of the patients [5,6]. The expression is evaluated immunohistochemically and the specific antibody to Ha-ras p21 was originally developed against a peptide of the C-terminal region [5,7]. Recently, a commercial antibody [Ha-ras(C-20), Santa Cruz, CA, USA] is available with same specificity to our antibody. We reported that the immunohistochemical expression of trk A also associated closely with clinical outcome of the patients [8] and was independent from the Ha-ras expression. Moreover, the combination of Ha-ras and trk A expression was useful to discriminate biological behavior of NBs [3]. Both Ha-ras and trk A genes associate closely with differentiation and apoptosis mechanism in NB cells, however, they function in different ways to cell death [9,10].

## 3. Evaluation of specificity and sensitivity of markers to clinical outcome

We focused the three markers, MYCN gene status, histopathology according to International Neuroblastoma Pathological Classification (INPC) [11] and Ha-ras/trk A expression for predicting clinical outcome of the patients [12]. First we evaluated retrospectively their predictive specificity and sensitivity to the clinical outcome (Fig. 1). The objective patients were diagnosed clinically (non-mass); 45 patients had clinical events such as progress, relapse and/or death and 42 were event-free survivors for more than 2 years after the diagnosis. Specificity to the poor clinical outcome was 86%(19/22) in NBs with MYCN amplification, 76%(25/33) in NBs with INPC unfavorable histology, and 75% (27/36) in NBs with low Ha-ras/trk A expression. However, the sensitivity to all 45 cases with poor clinical outcome were 42%(19/45), 55%(25/45), 60%(27/45) in NBs with MYCN amplification, INPC unfavorable histology and in low Ha-ras/trk A expression, respectively. Prognostic prediction by using one marker was insufficient because of the low sensitivity.

Therefore the three markers were combined for predicting risk to progress. NBs with any of the three markers, MYCN amplification, INPC unfavorable histology or low Ha-ras/trk A expression, increased the sensitivity to poor clinical outcome of the patients to 84% (38/45) and the specificity to poor clinical outcome was 73% (38/52).

On the other hand, NBs with all of three markers, such as 'single copy of MYCN' and 'INCP favorable histology' and 'high Ha-ras/trk A expression', showed quite favorable outcome of the patients. The specificity of the NBs to the good clinical outcome was 88%(22/25). We could predict the risk with high sensitivity and specificity.

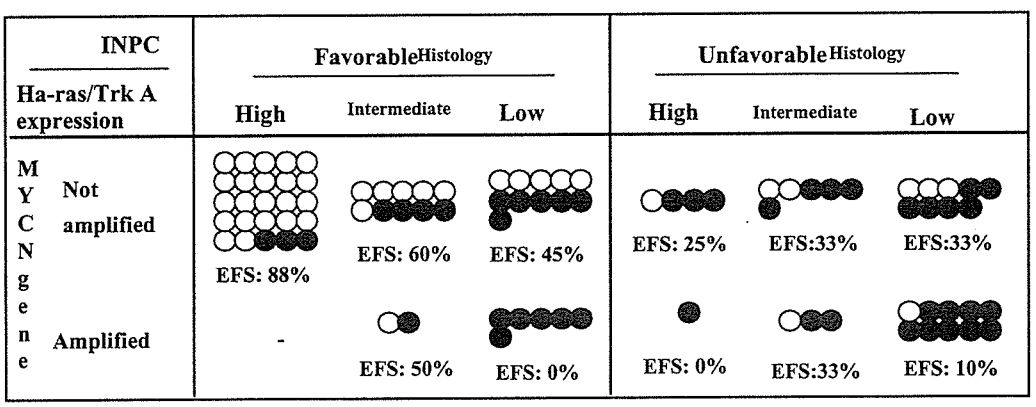


Fig. 1. Clinical outcome of the patients with neuroblastoma. All neuroblastomas were diagnosed clinically (non-massNBs). Open circle presents an event-free survivor and closed circle presents a patient with clinical events, such as death, relapse and progress. *Abbreviations*: INPC, International Neuroblastoma Pathological Classification; EFS, event-free survival rate.

## 4. Intervention in early stages salvages the patients with risk to progress

In our data base there were 94 NBs with at least one of the risk markers mentioned above. The event-free survival of the patients was 43% (40/94). Even with the cytogenetic markers, event-free survival was 86% in the patients with the localized NBs (stage I or II). On the other hand, the survival was 35% in the patients with advanced NBs (stage III, IVs or IV). This finding reveals that intervention in early stages improves clinical outcome of the patients, even if the NBs have risk to progress.

## 5. Clinical risk of the NBs defined by multivariate markers

Based on the results mentioned above, the '*high risk*' is defined by NBs in any stage with any of following markers, MYCN amplification or INPC unfavorable histology or low Ha-ras/trk A expression. The '*low risk*' is defined by NBs with all another markers, single copy of MYCN and INPC favorable histology and high Ha-ras/trk A expression and localized tumor. The remaining NBs are defined in '*intermediate risk*' category.

## 6. Estimation of biological profile in NBs detected through infantile mass-screening program

The Japanese mass-screening program was introduced in 1984 for infants at 6 months of age. This program detected 2366 NBs (mass-NBs) until 2001. The event-free survival of patients is 98%. There have been controversial discussion about benefit of the mass-screening. Quebec [13] and German [14] studies reported that the mass-screening provided no effect on mortality caused by NBs. Recent Japanese nation-wide study showed significant reduction of mortality in mass-screening group comparing with children who did not have the mass-screening [15]. The biological analysis of the mass-NBs has not been conclusive. We have been evaluating the biological property of the 248 mass-NBs and following their clinical outcome. They were about 10% of all mass-NBs in Japan. Based on criteria in the

| INPC[a] & Ha-ras/trk A[b] Stage | "Favorable"[a] "High" / "Intermediate" / "Low"[b] | | | "Unfavorable"[a] "High" / "Intermediate" / "Low"[b] | | | total□ (EFS/UO)[c] |
|---|---|---|---|---|---|---|---|
| I | ⑩○○○ ○○○○○○ ○○▼▼ n n | ○○○○○○ ○○○○ n | ○○○○ ○▲▼▼ n | ○ | | ○○○ | 99□ (94/5) |
| II | ○○○○ ○○▲▼ n | ○○○○ ○○○▲▼ | ○ | ○○▼ | ○○ | ○ | 78□ (73/5) |
| IVs | ○○○○○ ○○N | ○○○○ | ○ | | | | 12□ (12/0) |
| III | ○○ ○n▼ | ○ ▲●n | ○○○○○ ○○○▼ n | ○○ | | ▼ | 46□ (41/5) |
| IV | ○○○○○ ○ | ○○ | | | ●N | ○▲▲● N NN | 13□ (9/4) |
| total□ (EFS/UO)[c] | 138□ (133/5) | 55□ (51/4) | 36□ (32/4) | 6□ (5/1) | 4□ (3/1) | 9□ (5/4) | 248□ (229/19) |

Fig. 2. Biological profiles of 248 mass-NBs. (a) International neuroblastoma pathological classificaion (INPC), (b) H-ras/trk A expression, c; number of event-free survival (EFS) and patients with unfavorable outcome (UO). *Patients outcome*: small open circle presents a event-free survivor and large one presents 10 event-free survivors. Closed circle is a deceased case. A downward closed triangle is a case with relapse NB and a upward closed triangle is a case with progressive NB. Capital 'N' presents MYCN amplification with more than 10 copies and small 'n' presents the amplification with 3–9 copies.

non-mass NBs mentioned above, the 248 mass-NBs were classified into risk categories. Seventy-one percent of them were detected as localized tumors (stage I and II) and 29% were in stages III, IVs and IV. The MYCN amplification was detected in only 13 mass-NBs (5%). The distribution of mass-NBs with MYCN amplification and the better event-free survival [69% (9/13)] of the patients might suggest the benefit of early detection and intervention through the mass-screening. Total 62 NBs (25%) were evaluated to have high-risk property; 55 had INPC unfavorable histology or low Ha-ras/trk A expression and seven had only the MYCN amplification as a risk marker. Among localized 103 NBs (stages I, II) with INPC favorable histology and high Ha-ras/trk A expression, 100 NBs (40%) were classified as *low-risk property* and the MYCN amplified 3 NBs moved to high risk group. The remaining 86 NBs (35%) in other categories were classified to be *Intermediate risk* (Fig. 2).

## 7. Conclusion

The multivariate evaluation showed the diversity of non-mass- and mass-NBs with variety risk to progress. The cytogenetic markers, MYCN, INPC histology and Ha-ras/trk A expression could predict the risk with high sensitivity and specificity.

## Acknowledgements

This study was supported by Grants-in-aid for Cancer Research (13–19, 16–17) and for Scientific Research (H16-Clinical Cancer Research-039) from the Ministry of Health, Labor and Welfare of Japan and by grants (14370250,15659249) from the Ministry of Education, Science, Sports and Culture

## References

[1] J.M. Maris, K.K. Matthay, Molecular biology of neuroblastoma, J. Clin. Oncol. 17 (1999) 2264–2279.

[2] R.C. Seeger, G.M. Brodeur, H. Sather, A. Dalton, S.E. Siegel, K.Y. Wong, D. Hammond, Association of multiple copies of the N-myc oncogene with rapid progression of neuroblastgomas, N. Engl J. Med. 313 (1985) 1111–1116.

[3] T. Tanaka, T. Sugimoto, T. Sawada, Prognostic discrimination among neuroblastomas according to Ha-ras/trk A gene expression, Cancer 83 (1998) 1626–1633.

[4] G.M. Brodeur, Neuroblastoma: biological insights into a clinical enigma, Nat. Rev. Cancer 3 (2003) 203–216.

[5] T. Tanaka, D.J. Slamon, H. Shimoda, C. Waki, Y. Kawaguchi, Y. Tanaka, N. Ida, Expression of Ha-ras oncogene products in human neuroblastomas and significant correlation with patient's prognosis, Cancer Res. 48 (1988) 1030–1034.

[6] T. Tanaka, D.J. Slamon, H. Shimada, H. Shimoda, T. Fujisawa, N. Ida, R.C. Seeger, A significant association of Ha-ras p21 in neuroblastoma cells with patient prognosis, Cancer 68 (1991) 1296–1302.

[7] T. Tanaka, D.J. Slamon, M.J. Cline, Efficient generation of antibodies to oncoproteins by using synthetic peptide antigens, Proc. Natl Acad. Sci. USA 82 (1985) 3400–3404.

[8] T. Tanaka, E. Hiyama, T. Sugimoto, T. Sawada, M. Tanabe, N. Ida, Trk A gene expression in neuroblastoma: the clinical significance of an immunohistochemical study, Cancer 76 (1995) 1086–1095.

[9] A. Nakagawara, M. Arima-Nakagawara, N.J. Scavarda, C.G. Azar, A.B. Canter, G.M. Brodeur, Association between high levels of expression of the trk gene and favorable outcome in human neuroblastoma, N. Engl J. Med. 328 (1993) 847–854.

[10] C. Kitanaka, K. Kato, R. Ijiri, K. Sakurada, A. Tomiyama, K. Noguchi, et al., Increased ras expression and caspase-independent neuroblastoma cell death: possible mechanism of spontaneous neuroblastoma regression, J. Natl Cancer Inst. 94 (2002) 358–368.

[11] H. Shimada, I. Ambros, L.P. Dehner, J. Hata, V.V. Joshi, B. Roald, et al., The international neuroblastoma pathology classification (the Shimada system), Cancer 86 (1999) 364–372.

[12] T. Tanaka, T. Iehara, T. Sugimoto, M. Hamasaki, S. Teramukai, Y. Tsuchida, et al., in: B. De Bernardi, A. Garaventa et al. (Eds.), Multivariate evaluation for heterogeneous neuroblastomas Advances in Neuroblastoma Research, Eleventh Conference, Genova (2004), p. 64.

[13] W.G. Wood, R.M. Gao, J.J. Shuster, L.L. Robinson, M. Bernstein, S. Weitzman, et al., Lemieux: Screening of infants and mortality due to neuroblastoma, N. Engl J. Med. 346 (2002) 1041–1046.

[14] F.H. Schilling, C. Spix, F. Berthold, R. Erttmann, N. Fehse, B. Hero, et al., Neuroblastoma screening at one year of age, N. Engl J. Med. 346 (2002) 1047–1053.

[15] K. Hayashi, T. Fujita, K. Katanoda, T. Sobue, M. Nishi, K. Yamamoto, in: B. De Bernardi, A. Garaventa et al. (Eds.), Effectiveness of Mass-screening program on neuroblastoma mortality in 1995–2000 birth cohort of Japan: nationwide neuroblastoma mortality study Advances in Neuroblastoma Research, Eleventh Conference, Genova (2004), p. 93.

Oncogene (2005) 24, 7156–7169

www.nature.com/onc

# UFD2a mediates the proteasomal turnover of p73 without promoting p73 ubiquitination

Mitsuchika Hosoda[1,2,3], Toshinori Ozaki[1,3], Kou Miyazaki[1], Syunji Hayashi[1,2], Kazushige Furuya[1], Ken-ichi Watanabe[2], Takahito Nakagawa[2], Takayuki Hanamoto[1], Satoru Todo[2] and Akira Nakagawara*[,1]

[1]*Division of Biochemistry, Chiba Cancer Center Research Institute, 666-2 Nitona, Chuoh-ku, Chiba 260- 8717, Japan;* [2]*Department of General Surgery, Hokkaido University School of Medicine, Sapporo 060-8638, Japan*

**p73 protein level is kept extremely low in mammalian cultured cells and its stability may be regulated by not only the ubiquitin/proteasome-dependent proteolysis but also through other unidentified mechanisms. Here, we found for the first time that p73 is physically as well as functionally associated with the U-box-type E3/E4 ubiquitin ligase UFD2a. The immunoprecipitation experiments demonstrated that this interaction is mediated by the COOH-terminal region of p73α containing SAM domain. During the cisplatin-induced apoptosis in SH-SY5Y neuroblastoma cells, p73α accumulated at a protein level, whereas the endogenous UFD2a was significantly reduced in response to cisplatin. Ectopic expression of UFD2a decreased the half-life of p73α in association with a significant inhibition of the p73α-mediated transactivation as well as proapoptotic activity. Downregulation of endogenous UFD2a by antisense strategy resulted in a remarkable accumulation of p73α. Unexpectedly, UFD2a-mediated degradation of p73α was sensitive to the proteasomal inhibitor, however, UFD2a did not affect the ubiquitination levels of p73α. Taken together, our present findings imply that UFD2a might promote the proteasomal turnover of p73 in a ubiquitination-independent manner, and also suggest that UFD2a might play an important role in the regulation of cisplatin-induced apoptosis mediated by p73.**
*Oncogene* (2005) **24,** 7156–7169. doi:10.1038/sj.onc.1208872; published online 19 September 2005

**Keywords:** E3 ligase; p53; p73; ubiquitin; UFD2a

## Introduction

p73, which is a recently discovered p53 family member (Kaghad *et al.*, 1997), binds to the p53-responsive elements found within the promoter regions of a variety of p53-target genes, thereby inducing cell cycle arrest and/or apoptosis in certain cancerous cells (for a review, see Melino *et al.*, 2002). In contrast to *p53*, *p73* gives rise to multiple splice variants with different COOH-terminal tails such as p73α and p73β (Melino *et al.*, 2002). These variants have a different transcriptional and biological property. In fact, the ability of p73β to transactivate the p53-responsive promoters as well as to limit cell growth was stronger than p73α (Jost *et al.*, 1997; De Laurenzi *et al.*, 1998; Ueda *et al.*, 1999). Deletion of the COOH-terminal end region of p73α restored its transactivation potential, suggesting that the COOH-terminal region of p73α not included in the β form exerts an inhibitory effect on its function (Ozaki *et al.*, 1999; Ueda *et al.*, 1999). In addition to the COOH-terminal regulatory region, only the α forms of p73 and p63 (another member of p53 family) contain a sterile α motif (SAM) domain, which might mediate protein–protein interactions (Chi *et al.*, 1999; Thanos and Bowie, 1999). Although the SAM domain has been found in a variety of cellular proteins closely involved in the developmental regulation (Schultz *et al.*, 1997; Thanos *et al.*, 1999), its functional role in the regulation of p73 and p63 remains unclear.

Yang *et al.* (2000) found an $NH_2$-terminally truncated form of p73 (ΔNp73) arising from an alternative promoter usage. ΔNp73, which lacks the $NH_2$-terminal transactivation domain, was expressed predominantly in mouse developing brain and sympathetic neurons and inhibited the p53-dependent neuronal apoptosis by acting as a dominant-negative inhibitor of p53 (Pozniak *et al.*, 2000). In addition to its function as a p53 antagonist, ΔNp73 also has a dominant-negative effect on the function of p73 (Yang *et al.*, 2000), indicating that the balance between intracellular levels of pro-apoptotic p73 and tumor-promoting ΔNp73 might determine the cell fate. We and others have recently shown that p73 directly transactivates ΔNp73 through the putative p53/p73-target element within the *ΔNp73* promoter region (Grob *et al.*, 2001; Nakagawa *et al.*, 2002; Zaika *et al.*, 2002), suggesting that there exists a negative feedback regulation of p73 by its own target ΔNp73.

It has been demonstrated that p73 is stabilized and its proapoptotic activity is enhanced in response to DNA damage such as cisplatin treatment in a pathway depending on nuclear nonreceptor tyrosine kinase c-Abl (Agami *et al.*, 1999; Gong *et al.*, 1999; Yuan *et al.*,

*Correspondence: A Nakagawara; E-mail: akiranak@chiba-cc.jp
[3]These authors contributed equally to this work
Received 22 February 2005; revised 16 May 2005; accepted 24 May 2005; published online 19 September 2005

1999). Ren *et al.* (2002) described that protein kinase Cδ catalytic fragment-mediated phosphorylation of p73 at Ser-289 is strongly associated with the accumulation of p73. Since the steady-state levels of p73 were increased in the presence of the proteasomal inhibitor, p73 stability may be regulated at least in part by the protein degradation process mediated by ubiquitin–proteasome pathway (Balint *et al.*, 1999). In contrast to p53, MDM2, which mediates the ubiquitination of p53 to trigger its rapid degradation by proteasome, was able to interact with the $NH_2$-terminal transactivation domain of p73 to inhibit its function; however, coexpression of MDM2 with p73 resulted in an accumulation of p73 (Zeng *et al.*, 1999). Thus, p73 stability is regulated by another protein with E3 ubiquitin protein ligase activity. Alternatively, Ohtsuka *et al.* (2003) found that the proteolytic degradation of p73 is promoted by cyclin G in a ubiquitination-independent manner.

UFD2a, a member of the U-box-type ubiquitin protein ligase family, was initially identified as an E4 ubiquitination factor, which catalyses the elongation of a polyubiquitin chain to allow the targeting of the polyubiquitinated substrate proteins for degradation by proteasome (Koegl *et al.*, 1999; Hatakeyama *et al.*, 2001). The predicted three-dimensional structure of the U-box resembles that of the RING finger, and UFD2a also acts as an E3 ubiquitin protein ligase (Hatakeyama *et al.*, 2001). Recently, we have found that human *UFD2a* gene is mapped to 1p36.2–p36.3, which is a locus for candidate tumor suppressor gene(s) of neuroblastoma and other cancers (Ohira *et al.*, 2000). However, our mutational analysis suggested that *UFD2a* is infrequently mutated in neuroblastoma and neuroblastoma-derived cell lines. In yeast, Ufd2 is implicated in cell survival under stress conditions (Koegl *et al.*, 1999). Upon apoptotic stimuli, UFD2a was cleaved by caspase 6 or granzyme B, and its enzymatic activity was significantly impaired, indicating that UFD2a might play an important role in apoptotic signaling (Mahoney *et al.*, 2002).

In this report, we showed for the first time that p73α physically interacts with UFD2a in cells. Ectopic expression of UFD2a led to a massive decrease in the levels of p73α in association with a significant reduction of the transactivation as well as proapoptotic function of p73α. Although the UFD2a-mediated proteolytic degradation of p73α was sensitive to the proteasomal inhibitor, UFD2a did not affect the ubiquitination levels of p73α. Our present results strongly indicate that UFD2a participates in the regulation of the steady-state level of p73, thereby modulating the cisplatin-mediated apoptotic response.

## Results

### *Expression of UFD2a*

UFD2a is an E3/E4 ubiquitin protein ligase, which contains a regulatory domain and a catalytic U-box at its $NH_2$- and COOH-terminal region, respectively (Figure 1a). The expression patterns of *UFD2a* mRNA in various human tissues were examined by Northern blot analysis. Consistent with the previous results (Mahoney *et al.*, 2002), *UFD2a* mRNA was expressed at higher levels in human adult heart, placenta and skeletal muscle, whereas adult lung, liver and kidney had low to undetectable levels of *UFD2a* mRNA on Northern blot (Figure 1b). In addition, we found that the expression level of *UFD2a* mRNA was substantially higher in fetal tissues than in their corresponding adult ones. To examine the levels of endogenous UFD2a protein in a variety of mammalian cultured cells, we have generated a polyclonal antibody against the amino-acid sequence in the $NH_2$-terminal region of human UFD2a (amino acids 2–149), and analysed the steady-state levels of UFD2a by immunoblotting. Our antibody did not detect the endogenous UFD2a in whole lysates from NB-C201 human neuroblastoma cell line in which

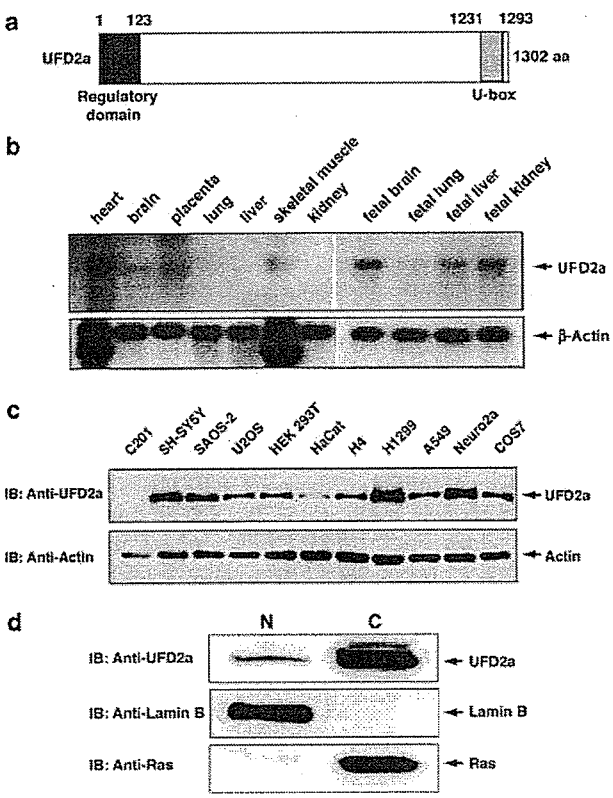


**Figure 1** Expression of *UFD2a* gene. (**a**) Schematic representation of human UFD2a. $NH_2$-terminal regulatory domain and COOH-terminal U-box are indicated. (**b**) Human multiple tissue Northern blot containing poly(A)$^+$RNA was hybridized with the radiolabeled human *UFD2a* cDNA. The ~5 kb transcript is shown. Relative RNA loading is shown below by reprobing the membrane with a probe specific for *β-actin*. α- or *γ-actin* accounts for the faster-migrating band. (**c**) Immunoblot analysis of UFD2a expression. Whole lysates (50 μg/lane) prepared from the indicated cell lines were separated by a 7.5% SDS–PAGE followed by immunoblotting with the anti-UFD2a antibody (top panel). Equal loading was verified by stripping and reprobing the blot with the anti-actin antibody (bottom panel). (**d**) Subcellular localization of endogenous UFD2a. The nuclear (N) and cytoplasmic (C) fractions were prepared from U2OS cells. Samples were loaded onto a 7.5% SDS–PAGE and subjected to immunoblotting with the anti-UFD2a (top panel), anti-Lamin B (middle panel) or anti-Ras (bottom panel) antibody

*UFD2a* gene is homozygously deleted (Ohira *et al.*, 2000) (Figure 1c). These observations suggest that our antibody is highly specific for UFD2a. Among cell lines, a higher level of expression was observed in SH-SY5Y, SAOS-2, H1299 and Neuro2a cells, and a relatively lower level of expression was detected in U2OS, HEK 293T, H4, A549 and COS7 cells. In accordance with the previous report (Mahoney *et al.*, 2002), the endogenous UFD2a was detected as a single anti-UFD2a reactive band migrating at ~130 kDa, and equal protein loading was confirmed by immunoblotting with an anti-actin antibody.

To determine the subcellular localization of the endogenous UFD2a, we used the biochemical cell fractionation procedure in U2OS cells. Equal amounts of cytoplasmic and nuclear fractions were subjected to immunoblotting with the anti-UFD2a antibody. Ras and Lamin B served as markers for the purity of the cytoplasmic and nuclear fractions, respectively. As described by Hatakeyama *et al.* (2001), UFD2a localized to both the cytoplasm and nucleus (Figure 1d).

### *Downregulation of UFD2a during the cisplatin-induced apoptosis*

The previous reports have shown that yeast Ufd2 is implicated in cell survival under stress conditions including exposure to the heavy metal cadmium and ethanol (Koegl *et al.*, 1999), and also showed that certain apoptotic stimuli induce the cleavage of human UFD2a by caspase 6 or granzyme B to reduce its enzymatic activity (Mahoney *et al.*, 2002), raising a possibility that UFD2a might participate in the regulation of proapoptotic proteins. To test this hypothesis, we first investigated the expression levels of UFD2a before and after DNA damage. As described (Nakagawa *et al.*, 2002), SH-SY5Y cells treated with cisplatin for 24 h underwent apoptosis in a dose-dependent manner as measured by cell survival assays (Figure 2a), and this apoptotic process was associated with a remarkable increase in proapoptotic p73α and its target $p21^{WAF1}$ at a protein level (Figure 2b). UFD2a was abundantly expressed in untreated SH-SY5Y cells; however, the level of UFD2a was significantly reduced in response to cisplatin treatment. To rule out the possibility that the intracellular level of UFD2a could be regulated at mRNA level, RT–PCR analysis was performed. As shown in Figure 2c, the expression level of *UFD2a* mRNA remained constant, regardless of cisplatin treatment. These results strongly suggest that the apoptotic signal brought about by cisplatin causes UFD2a downregulation in association with the significant stabilization of p73, and UFD2a might play an important role in the regulation of p73 stability.

### *Physical interaction of UFD2a with p73*

We assessed whether UFD2a could interact with p73 in cells. COS7 cells were transiently transfected with an expression plasmid for FLAG-tagged p73α, and whole lysates were subjected to immunoprecipitation with the anti-UFD2a antibody or with a normal rabbit serum (NRS) followed by immunoblotting with the anti-UFD2a antibody or with an antibody against p73. As shown in Figure 3a, the anti-UFD2a immunoprecipitates contained the endogenous UFD2a as well as FLAG-p73α. In addition, immunoprecipitation of FLAG-p73α resulted in the coprecipitation of the endogenous UFD2a, confirming that UFD2a and p73α are members of the same protein complex. On the other hand, UFD2a did not coimmunoprecipitate with p53 under our experimental conditions (Figure 3b). Due to the quality of the anti-p73 antibody that we used and/or the extremely low level of p73 in cells, we did not

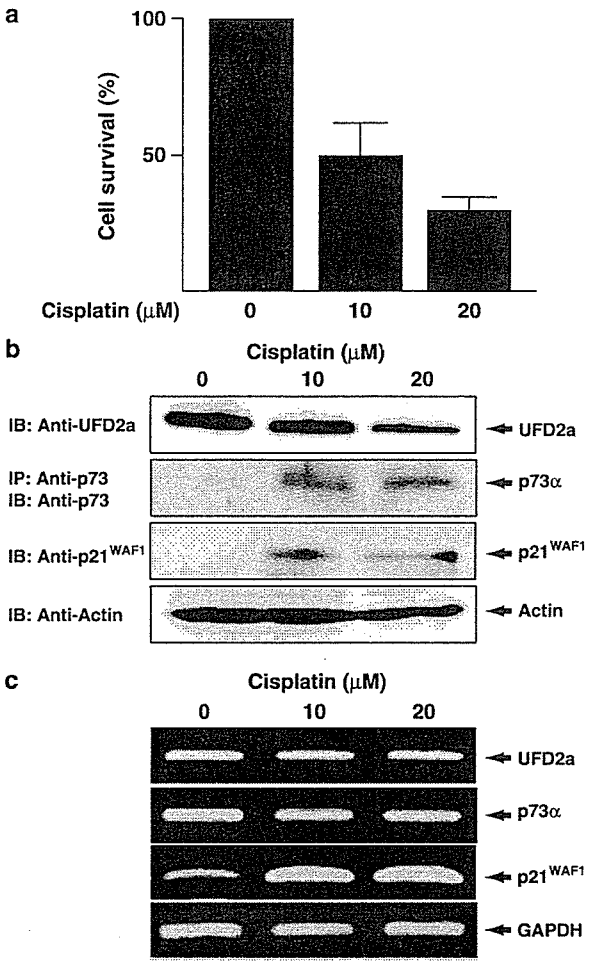


**Figure 2** Downregulation of UFD2a in response to cisplatin. (**a**) Cell survival assays of SH-SY5Y cells exposed to increasing amounts of cisplatin for 24 h. Data are presented as the mean value±standard deviation (s.d.) of at least six independent experiments. (**b**) Immunoblot analysis. SH-SY5Y cells were cultured in the absence or presence of the indicated concentrations of cisplatin for 24 h. Whole lysates were prepared from each culture and subjected to immunoblotting with the antibody specific for UFD2a (first panel), p73 (second panel) or $p21^{WAF1}$ (third panel). Equal loading was checked with anti-actin antibody (fourth panel). (**c**) RT–PCR analysis. Total RNA prepared from SH-SY5Y cells exposed to the indicated concentrations of cisplatin for 24 h was subjected to RT–PCR. *GAPDH* was used as a loading control (bottom panel)

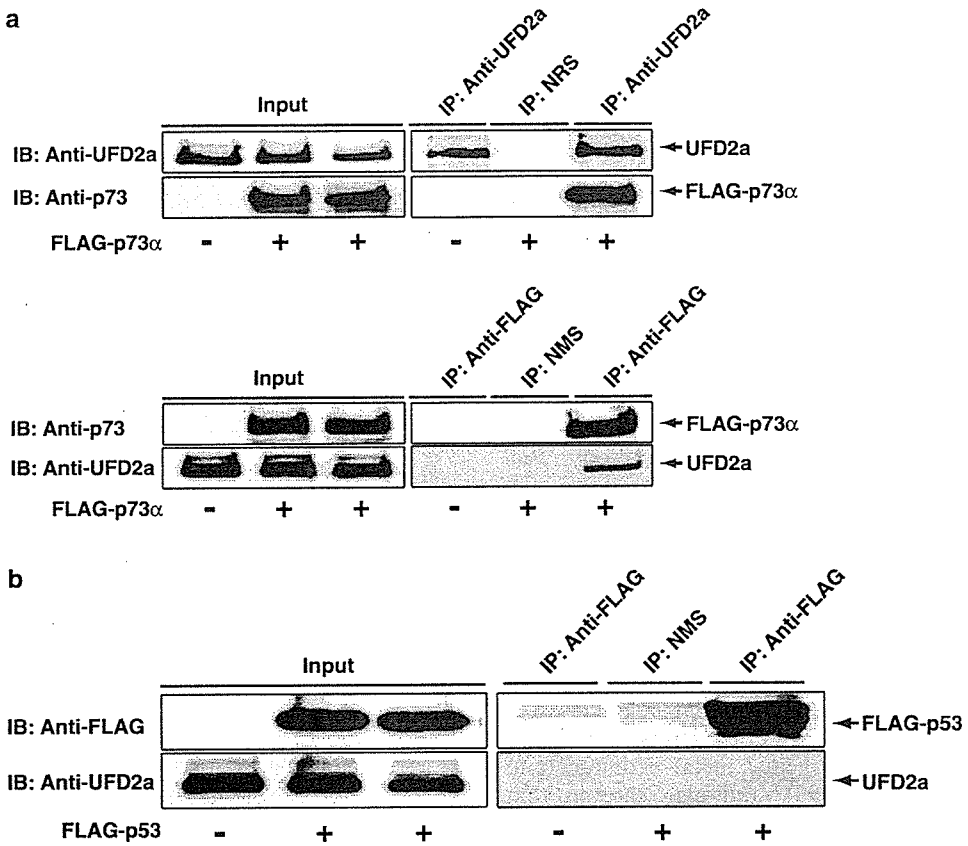


**Figure 3** Complex formation between UFD2a and p73. (**a**) p73α interacts with UFD2a in cells. In the upper panels, whole lysates from COS7 cells transiently transfected with the empty plasmid or with the expression plasmid for FLAG-tagged p73α were immunoprecipitated with the anti-UFD2a antibody or with NRS. Immunoprecipitates were analysed by immunoblotting with the anti-UFD2a (top panel) or anti-p73 (bottom panel) antibody. In the lower panels, the same lysates were immunoprecipitated with the anti-FLAG antibody or with a normal mouse serum (NMS). Immunoprecipitates were analysed by immunoblotting with the anti-p73 (top panel) or anti-UFD2a (bottom panel) antibody. (**b**) p53 does not interact with UFD2a. COS7 cells were transiently transfected with the empty plasmid or FLAG-p53 expression plasmid. Whole lysates were subjected to immunoprecipitation with the anti-FLAG antibody or NMS. Immunoprecipitates were analysed by immunoblotting with the anti-FLAG (top panel) or anti-UFD2a (bottom panel) antibody

detect the complex formation between the endogenous p73α and UFD2a.

### *SAM domain of p73 is required for interaction with UFD2a*

To identify the region(s) of p73 required for the interaction with UFD2a, we expressed a series of p73α deletion mutants as well as p73β in COS7 cells, and examined their abilities to interact with the endogenous UFD2a by coimmunoprecipitation experiments. Their structures are shown in Figure 4a. As reported previously (Ozaki *et al*., 1999), HA-p73α (1–427) and HA-p73α (1–548) localized to cell nucleus, whereas HA-p73α (1–247) was detected in both cell nucleus and cytoplasm (data not shown). As shown in Figure 4b and c, all of the p73 proteins, with the exception of p73α (1–548), which retains the SAM domain, were not detected in the anti-UFD2a immunoprecipitates, suggesting that the p73α COOH-terminal region containing SAM domain is required for the interaction with UFD2a.

### *UFD2a interferes with the steady-state level of p73α but not of p53*

To examine a possible effect of UFD2a on p73 stability, U2OS cells were cotransfected with a constant amount of the expression plasmid encoding HA-p73α, HA-p73β or FLAG-p53 together with or without increasing amounts of the FLAG-UFD2a expression plasmid. As shown in Figure 5a, enforced expression of FLAG-UFD2a greatly reduced the levels of HA-p73α in a dose-dependent manner. As expected, FLAG-UFD2a had marginal effects on the levels of HA-p73β and FLAG-p53, which did not bind to UFD2a (Figure 5b and c), suggesting that UFD2a specifically promotes the downregulation of p73α. We next sought to investigate the effect of UFD2a on the endogenous p73α. COS7 cells were transfected with or without increasing amounts of the FLAG-UFD2a expression plasmid, and were subsequently treated with cisplatin or left untreated. Consistent with the previous observations (Tsai and Yuan, 2003), the endogenous p73α

was stabilized in response to cisplatin (Figure 5d). Of note, overexpression of FLAG-UFD2a resulted in a significant inhibition of the cisplatin-mediated accumulation of p73α. Additionally, FLAG-UFD2a had an undetectable effect on the expression level of p73α mRNA.

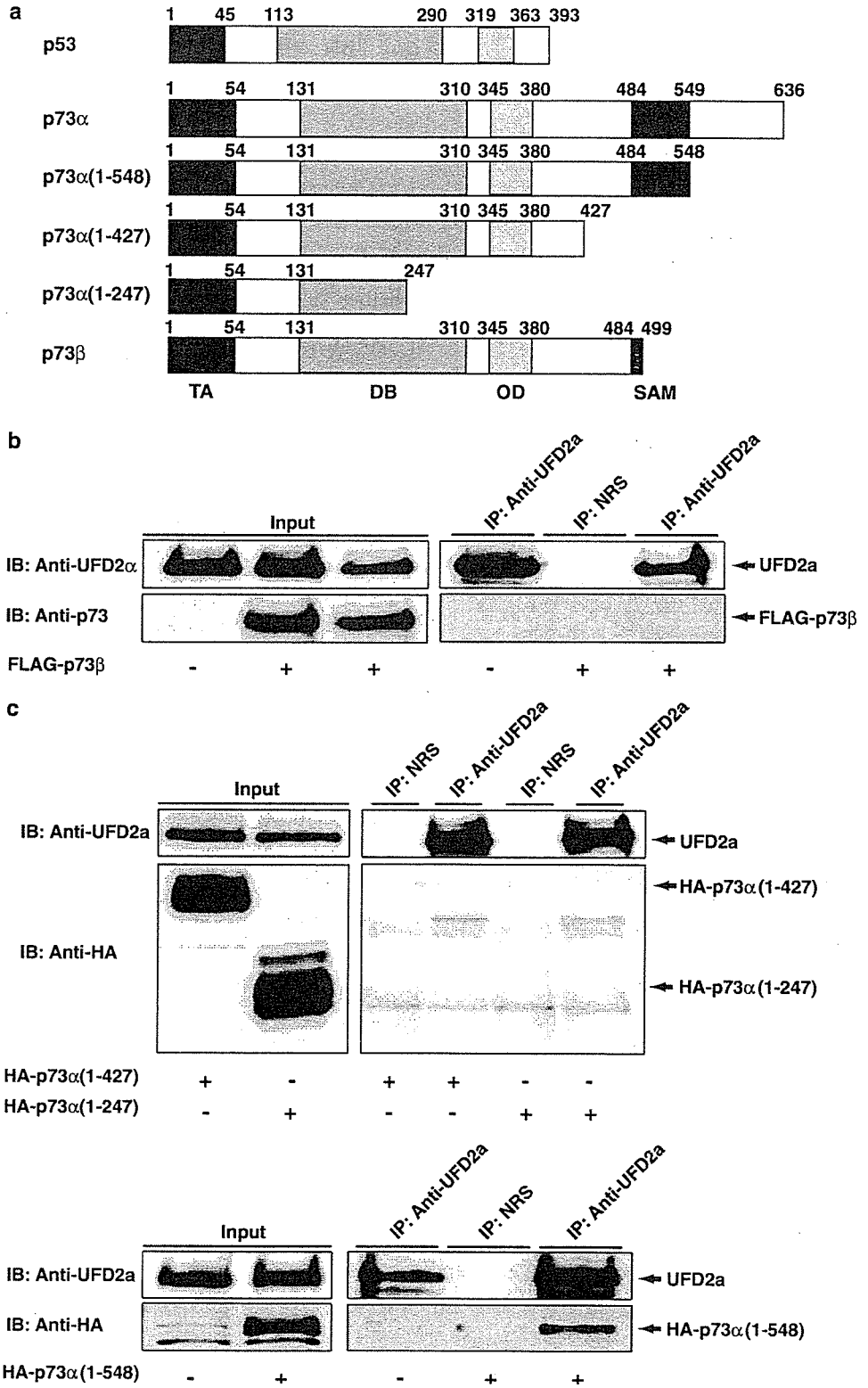

To determine whether UFD2a could affect the half-life of p73, U2OS cells were cotransfected with the expression plasmid for HA-p73α together with or without the FLAG-UFD2a expression plasmid. At 24 h after transfection, cells were treated with cycloheximide (at a final concentration of 20 μg/ml), which inhibits *de novo* protein synthesis. At the indicated time points following cycloheximide treatment, cells were collected, and whole lysates were analysed for the expression levels of HA-p73α by immunoblotting. As shown in Figure 6a and b, HA-p73α decayed at faster rates in the presence of FLAG-UFD2a than in its absence, whereas the coexpression of FLAG-UFD2a had little effect on the half-life of FLAG-p53. In addition, the half-life of the exogenously expressed HA-p73β was not affected by FLAG-UFD2a (data not shown).

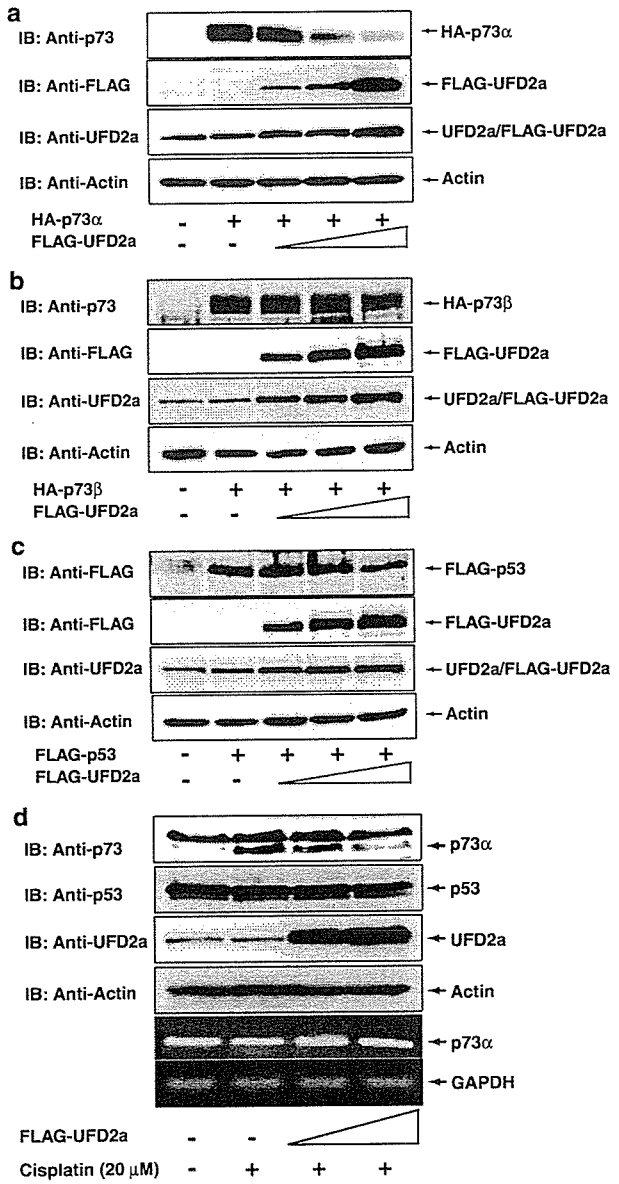


**Figure 5** UFD2a decreases the stability of p73α. (**a–c**) Effect of UFD2a on the expression levels of p73α, p73β and p53. U2OS cells were transiently cotransfected with 0.5 μg of the expression plasmid for HA-p73α (**a**), HA-p73β (**b**) or FLAG-p53 (**c**) together with or without increasing amounts of FLAG-UFD2a expression plasmid (0.5, 1.0 and 1.5 μg). At 48 h after transfection, whole lysates were prepared and analysed by immunoblotting with the indicated antibodies. To control for equal amounts of protein loading, levels of actin were monitored by immunoblotting (bottom panels). (**d**) UFD2a inhibits the cisplatin-mediated stabilization of endogenous p73α. COS7 cells were transiently transfected with the empty plasmid or with the expression plasmid for FLAG-UFD2a. At 24 h after transfection, cells were treated with 20 μM of cisplatin for 24 h or left untreated, and whole lysates (upper panels) and total RNA (lower panels) were analysed by immunoblotting and RT–PCR, respectively

### *UFD2a-mediated degradation of p73α is regulated in a ubiquitination-independent manner*

The results presented on the role of UFD2a in the negative regulation of p73α prompted us to examine whether a ubiquitin–proteasome pathway could be involved in this process. In order to verify this idea, U2OS cells expressing HA-p73α and FLAG-UFD2a were treated with a potent inhibitor of proteasome function, MG-132. As shown in Figure 7a, the UFD2a-mediated reduction of HA-p73α was restored to a level close to the control in the presence of MG-132. Next, we performed the ubiquitination assays. U2OS cells were transiently cotransfected with the expression plasmid for HA-p73α and hexahistidine (His)-tagged ubiquitin together with or without increasing amounts of the FLAG-UFD2a expression plasmid. At 48 h after transfection, cells were exposed to MG-132 for 6 h. Ubiquitinated proteins were isolated by nickel-agarose beads, and then analysed by immunoblotting with the anti-HA antibody. Under our experimental conditions, coexpression of p53 with MDM2 resulted in a remarkable increase in the p53 ubiquitination levels (data not

**Figure 4** SAM domain of p73α is required for the interaction with UFD2a. (**a**) Schematic diagram of p73, p53 and the deletion mutants of p73. TA (transactivation), DB (DNA-binding), OD (oligomerization) and SAM (sterile α motif) domains are indicated. (**b**) p73β does not bind to UFD2a. COS7 cells were transiently transfected with the empty plasmid or with the expression plasmid for FLAG-p73β. Whole lysates were subjected to immunoprecipitation with the anti-UFD2a antibody or with NRS followed by immunoblotting with the anti-UFD2a (top panel) or with the anti-p73 (bottom panel) antibody. (**c**) Anti-UFD2a immunoprecipitates contain p73α (1–548), but not p73α (1–427), and p73α (1–247). Whole lysates from COS7 cells transiently transfected with the expression plasmid for HA-p73α (1–247), HA-p73α (1–427) or HA-p73α (1–548) were immunoprecipitated with the anti-UFD2a antibody or with NRS and the immunoprecipitates were analysed by immunoblotting with the anti-HA antibody

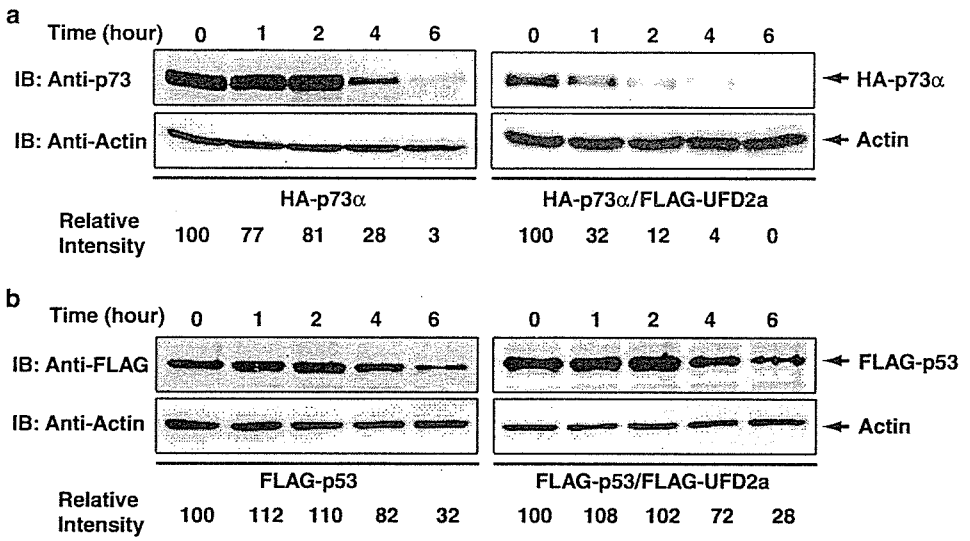


**Figure 6** UFD2a decreases the half-life of p73α. (**a**, **b**) U2OS cells were transiently cotransfected with 0.5 μg of the plasmid expressing HA-p73α (**a**) or FLAG-p53 (**b**) together with or without 1.5 μg of the expression plasmid for FLAG-UFD2a. At 24 h after transfection, cycloheximide was added to the culture medium (20 μg/ml), and whole lysates were prepared at the indicated time points. The levels of HA-p73α and FLAG-p53 were analysed by immunoblotting with the anti-p73 and anti-FLAG antibodies, respectively. Densitometry was used to quantify the amounts of HA-p73α or FLAG-p53, which normalized to actin, and band intensity of HA-p73α or FLAG-p53 was calculated against the amount of HA-p73α or FLAG-p53 present at time point 0, which was set at 100%

shown). In good agreement with the recent report (Bernassola *et al.*, 2004), we observed the appearance of the higher molecular weight ubiquitin-conjugated p73α in the presence of His-ubiquitin (Figure 7b). Unexpectedly, the amounts of the ubiquitinated p73α remained unchanged even in the presence of FLAG-UFD2a. As described previously (Hatakeyama *et al.*, 2001), the COOH-terminal U-box of UFD2a was required for its E3 ubiquitin ligase activity. We have constructed the FLAG-tagged deletion mutant of UFD2a (FLAG-UFD2aΔ), which lacks the COOH-terminal U-box, and examined whether it could reduce the level of p73α. As shown in Figure 7c, FLAG-UFD2aΔ retained an ability to downregulate p73α. Collectively, these results strongly suggest that UFD2a accelerates the proteasomal turnover of p73α in a ubiquitination-independent manner.

### *UFD2a reduces the p73α-dependent transcriptional activity and proapoptotic function*

To further investigate the functional consequences of the interaction between UFD2a and p73α, we tested the effect of FLAG-UFD2a on the p73α-dependent transcriptional activation in p53-deficient human lung carcinoma H1299 cells. As seen in Figure 8a, the enforced expression of HA-p73α resulted in a remarkable induction of the endogenous $p21^{WAF1}$, and coexpression of FLAG-UFD2a with HA-p73α decreased the levels of HA-p73α in association with a significant downregulation of the endogenous $p21^{WAF1}$. In contrast, FLAG-UFD2a had no obvious effects on the p53-mediated upregulation of the endogenous $p21^{WAF1}$ (Figure 8b).

We next examined a possible effect of UFD2a on the p73α-mediated apoptosis. H1299 cells were transiently cotransfected with a constant amount of the GFP expression plasmid and the expression plasmid for HA-p73α or FLAG-p53 together with or without the FLAG-UFD2a expression plasmid. At 48 h post-transfection, transfected cells were scored by fluorescence microscopy for the appearance of green fluorescence, and the number of GFP-positive cells with condensed and fragmented nuclei was counted. Overexpression of HA-p73α or p53 led to an increase in the number of apoptotic cells as compared with the control transfection (Figure 8c). Intriguingly, coexpression of HA-p73α with FLAG-UFD2a decreased the number of apoptotic cells as compared with that resulting from expression of HA-p73α alone. In contrast, FLAG-UFD2a had an undetectable effect on the p53-mediated apoptosis.

### *Antisense UFD2a enhances the function of p73α*

To characterize the effect of the endogenous UFD2a on p73α, we employed antisense strategy to reduce the endogenous UFD2a expression and function. For this purpose, H1299 cells were transiently transfected with an antisense *UFD2a* expression plasmid (As-*UFD2a*). At 48 h after transfection, the endogenous levels of UFD2a were analysed by immunoblotting. As shown in Figure 9a, the expression of the antisense *UFD2a* resulted in a significant decrease in UFD2a protein (left panels). Additionally, coexpression of HA-p73α with the antisense *UFD2a* led to an increase in the amount of HA-p73α (right panels). H1299 cells were then transiently cotransfected with a constant amount of the expression plasmid for HA-p73α or HA-p73β, together

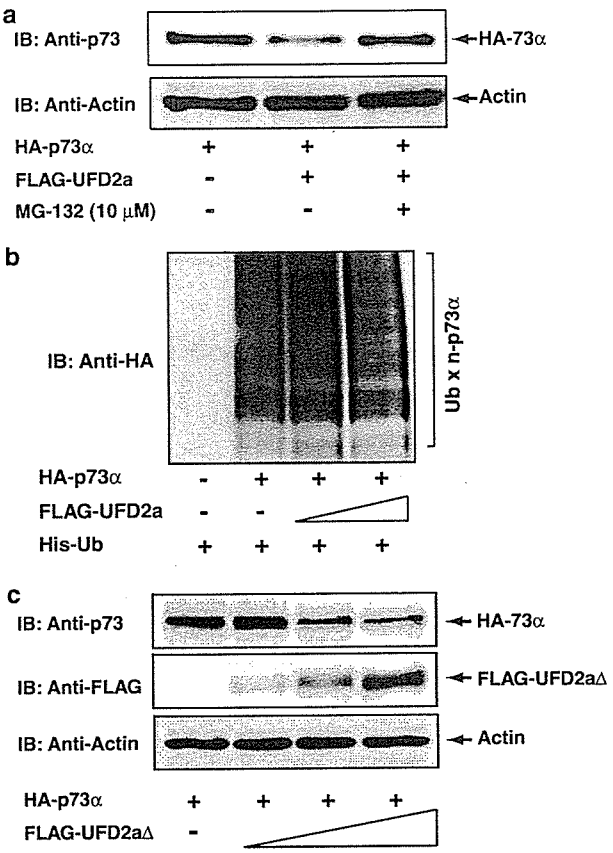


**Figure 7** UFD2a promotes p73α proteasomal turnover in a ubiquitination-independent manner. (**a**) Effect of proteasomal inhibitor on the UFD2a-mediated degradation of p73α. U2OS cells were transiently cotransfected with 0.5 μg of the HA-p73α expression plasmid together with or without 1.5 μg of the expression plasmid for FLAG-UFD2a. At 24 h after transfection, cells were left untreated or treated with MG-132 (10 μM) for 6 h, and whole lysates were analysed by immunoblotting with the anti-p73 antibody. Actin was used as a loading control (bottom panel). (**b**) UFD2a does not increase the ubiquitination levels of p73α. U2OS cells were transiently cotransfected with the indicated combinations of the expression plasmids. At 48 h after transfection, cells were treated with MG-132 for 6 h. Ubiquitinated materials were then isolated by nickel-agarose beads, and analysed by immunoblotting with the anti- HA antibody. (**c**) Enzymatic activity of UFD2a is not required for the downregulation of p73α. U2OS cells were transiently cotransfected with a constant amount of the expression plasmid for HA-p73α (0.5 μg) together with or without increasing amounts of the FLAG-UFD2aΔ expression plasmid (0.5, 1.0 and 1.5 μg). At 48 h after transfection, whole lysates were prepared and analysed for HA-p73α. Actin was used as a loading control

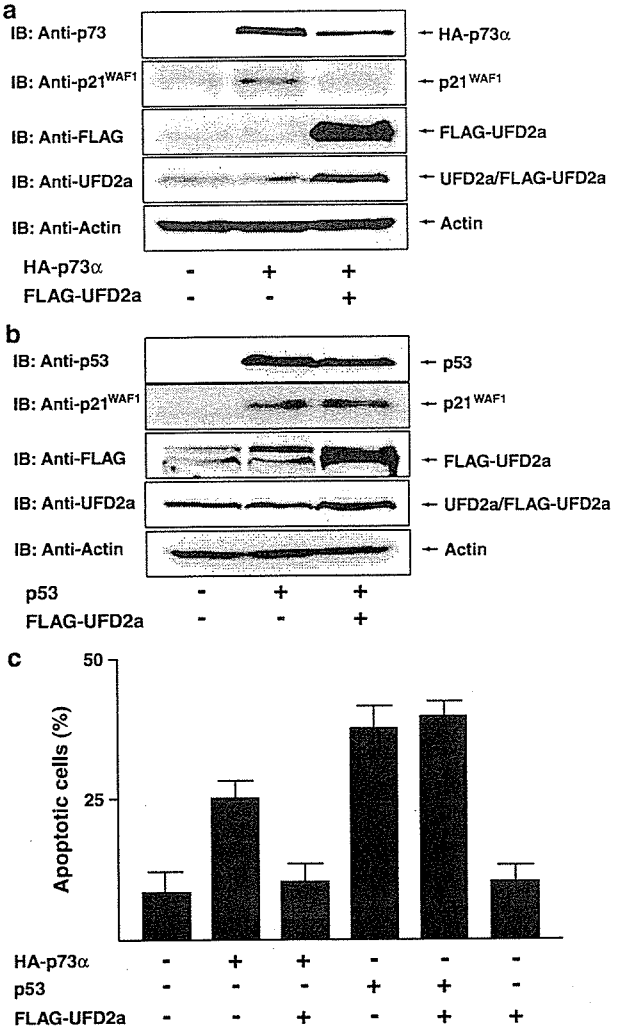


**Figure 8** UFD2a inhibits the p73α-mediated transactivation and proapoptotic functions. (**a**, **b**) UFD2a specifically attenuates the p73α-mediated upregulation of $p21^{WAF1}$. p53-deficient H1299 cells were transiently cotransfected with 0.5 μg of the expression plasmid encoding HA-p73α (**a**) or p53 (**b**) together with or without 1.5 μg of the FLAG-UFD2a expression plasmid. At 48 h after transfection, whole lysates were analysed by immunoblotting with the indicated antibodies. Actin was used as a loading control (bottom panel). (**c**) UFD2a inhibits the proapoptotic activity of p73α but not of p53. H1299 cells were transiently cotransfected with the indicated combinations of the expression plasmids. A constant amount of the GFP expression plasmid (200 ng) was included in all the combinations, and the total amount of plasmid DNA was kept constant (2 μg) by including an appropriate amount of empty plasmid. At 48 h post-transfection, transfected cells were identified by the presence of green fluorescence. Cell nucleus was stained with DAPI to reveal nuclear condensation and fragmentation. The number of GFP-positive cells with condensed and fragmented nuclei was scored, and the percentage of apoptotic cells shown in each column represents the mean of three independent experiments

with the p53/p73-responsive luciferase reporter construct containing *$p21^{WAF1}$* or *Bax* promoter in the presence or absence of As-*UFD2a*. As shown in Figure 9b, the expression of the antisense *UFD2a* caused a significant enhancement of the ability of p73α to drive transcription from *$p21^{WAF1}$* or *Bax* promoter. In contrast, coexpression of the antisense *UFD2a* with p73β resulted in only a marginal effect on the p73β-mediated transactivation (Figure 9c). Similar results were also obtained in p53-deficient SAOS-2 cells (data not shown). Consistent with these results, cotransfection of HA-p73α with the antisense *UFD2a* in H1299 cells induced the endogenous $p21^{WAF1}$ compared with that in cells expressing HA-p73α alone (Figure 9d). These findings collectively demonstrated that the reduction of

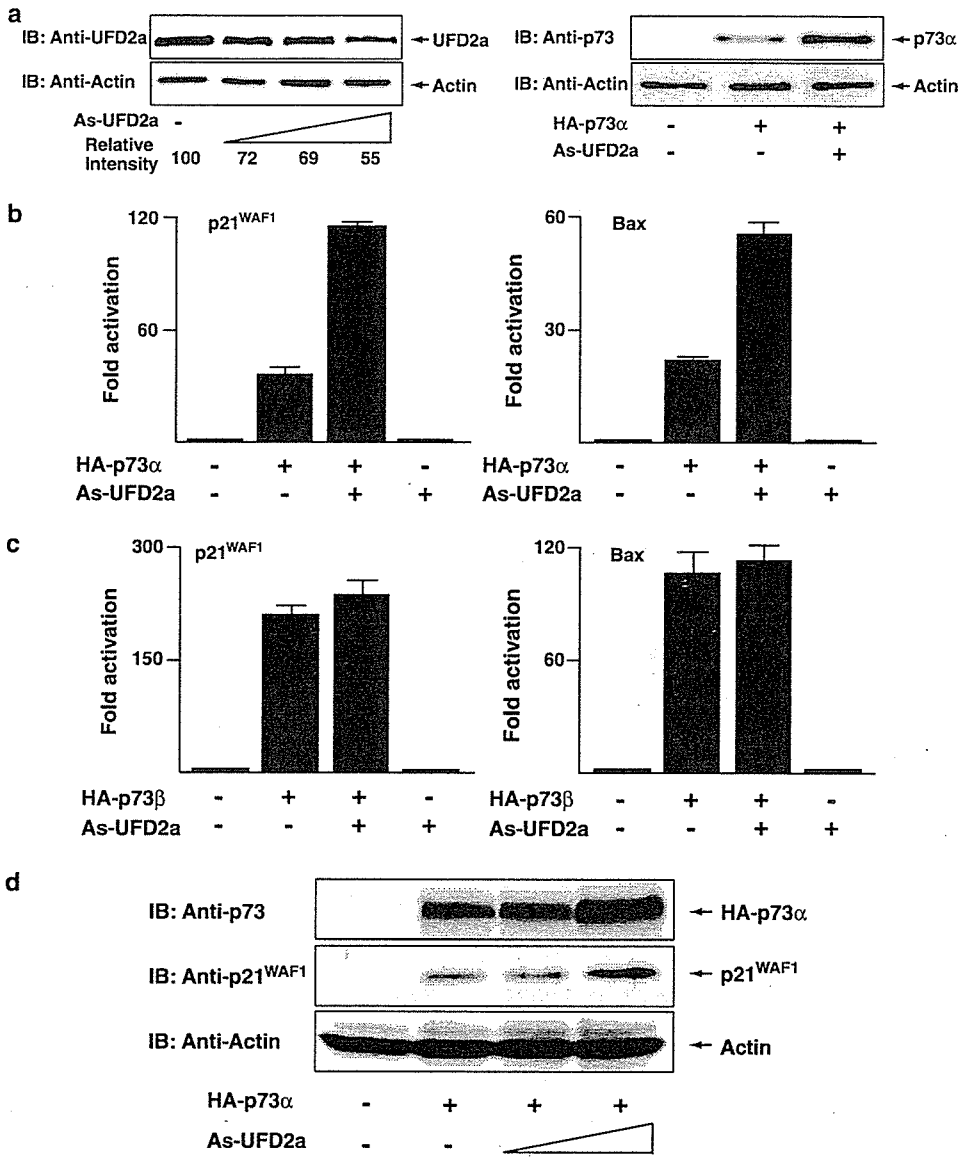


**Figure 9** Antisense *UFD2a* enhances the p73α-mediated transcriptional activity. (**a**) Antisense *UFD2a* expression in H1299 cells results in a reduction of endogenous UFD2a. Left panels: H1299 cells were transiently transfected with or without increasing amounts of the antisense *UFD2a* expression plasmid (As-*UFD2a*) (0.5, 1.0 and 1.5 μg). Whole lysates were prepared and subjected to immunoblotting with the anti-UFD2a antibody (top panel). Immunoblotting for actin is shown as control for protein loading (bottom panel). Densitometry was used to quantify the amounts of UFD2a, which normalized to actin. Right panels: H1299 cells were transiently cotransfected with 0.5 μg of the HA-p73α expression plasmid along with or without 1.5 μg of As-*UFD2a*, and whole lysates were analysed by immunoblotting with the indicated antibodies. (**b**, **c**) Antisense *UFD2a* enhances the transcriptional activity of p73α but not of p73β. H1299 cells were transiently cotransfected with 25 ng of the expression plasmid for HA-p73α (**b**) or HA-p73β (**c**) together with the p53/p73-responsive luciferase reporter constructs (100 ng) as indicated, and 10 ng of the *Renilla* luciferase plasmid (pRL-TK) in the presence or absence of the antisense *UFD2a* expression plasmid (200 ng). Total amounts of plasmid DNA per transfection were kept constant (510 ng) with pcDNA3. At 48 h after transfection, the firefly luciferase activities were determined. The transfection efficiency was standardized against *Renilla* luciferase. Results shown are representative of three independent experiments. (**d**) Downregulation of the endogenous UFD2a results in an enhancement of the p73α-dependent induction of $p21^{WAF1}$. Whole lysates prepared from H1299 cells transiently cotransfected with the expression plasmid for HA-p73α (0.5 μg) in the presence or absence of increasing amounts of As-*UFD2a* (0.5 and 1.5 μg) were analysed by immunoblotting with the indicated antibodies. Actin was used as a loading control (bottom panel)

the endogenous UFD2a enhances the transactivation ability of p73α.

We next determined a possible effect of antisense *UFD2a* expression on the p73α-mediated growth suppression. H1299 cells were cotransfected with the expression plasmid for HA-p73α or HA-p73β in the presence or absence of increasing amounts of the antisense *UFD2a* construct, and cultured in the presence

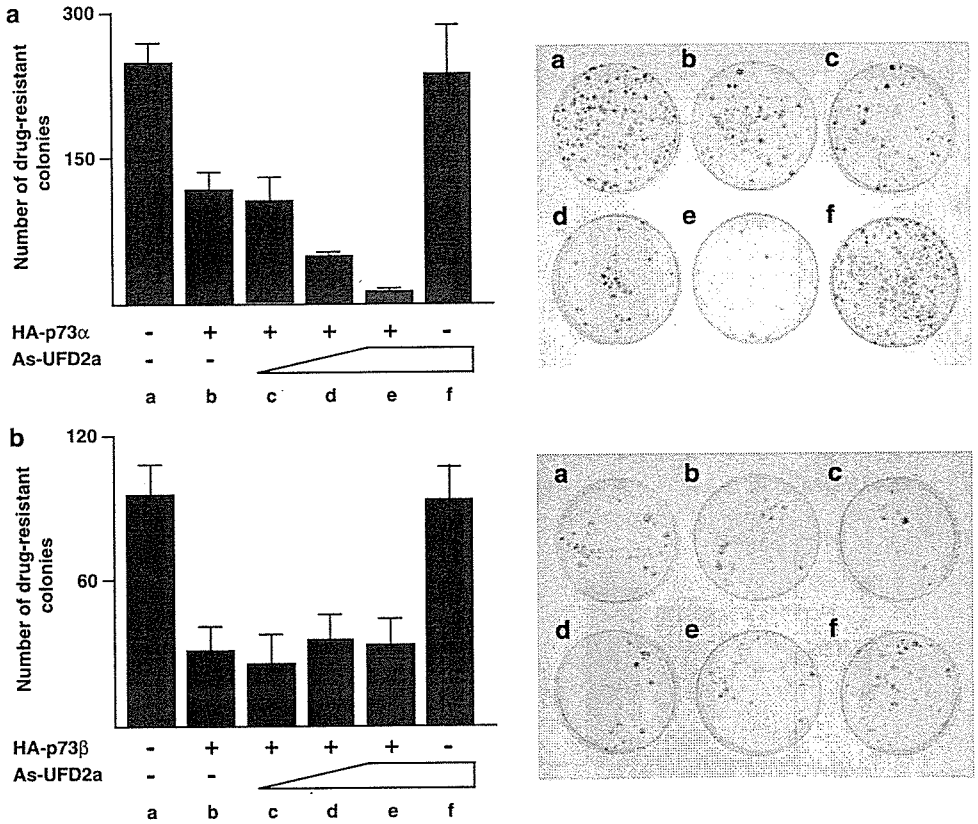


**Figure 10** Colony formation assay. (**a**, **b**) H1299 cells were transfected with a constant amount of the expression plasmid (200 ng) for HA-p73α (**a**) or HA-p73β (**b**) along with or without increasing amounts of the antisense *UFD2a* expression plasmid (200, 400 and 800 ng) (As-*UFD2a*). Total amounts of plasmid DNA per transfection were kept constant (1 μg) with pcDNA3. At 48 h after transfection, cells were split and kept in the medium containing G418 (400 μg/ml), and surviving colonies were counted after 2 weeks

of G418 (400 μg/ml) for 2 weeks. As shown in Figure 10a and b, coexpression of the antisense *UFD2a* with HA-p73α resulted in a remarkable reduction in the number of drug-resistant colonies compared with cells transfected with HA-p73α alone, whereas the antisense *UFD2a* had no significant effect on the growth inhibitory activity of p73β. Taken together, these results indicated that UFD2a destabilizes p73α, thereby reduces its transactivation and proapoptotic activities.

## Discussion

UFD2a is a newly identified mammalian homolog of yeast Ufd2 (Koegl *et al*., 1999). UFD2a contains a U-box at its COOH-terminus whose predicted three-dimensional structure is similar to that of RING finger domain of E3 ubiquitin protein ligases, and in fact it functions as E3 as well as E4 ubiquitin protein ligase, which generates polyubiquitin conjugates from mono-ubiquitinated substrate proteins (Koegl *et al*., 1999; Hatakeyama *et al*., 2001). Immunohistochemical analysis revealed that UFD2a is expressed predominantly in mouse neuronal tissues, suggesting that UFD2a contributes to the ubiquitination of specific target protein(s) involved in neuronal function (Kaneko *et al*., 2003), although its physiological substrate(s) remains to be identified. In the present study, we have demonstrated that UFD2a binds to p73α and this interaction relies on the p73α COOH-terminal region containing SAM domain. Our results also indicated that UFD2a mediates the proteolytic degradation of p73α but not of p53, thereby inhibiting its transactivation as well as pro-apoptotic activity in cells. Of note, the UFD2a-mediated degradation of p73α was sensitive to the proteasomal inhibitor, however, this degradation process was not associated with the increase in the ubiquitination levels of p73α. Upon cisplatin treatment in SH-SY5Y cells, the endogenous UFD2a was reduced, thereby allowing the accumulation of p73α. Thus, our findings provide an insight into the ubiquitination-independent mechanism for UFD2a-mediated proteolysis of its target proteins such as p73α, although further investigation should be required to clarify the precise molecular mechanism underlying the UFD2a-mediated degradation of p73α.

MDM2 promotes the ubiquitination and subsequent degradation of p53 by proteasome, and disruption of the interaction between them is a key event for p53 stabilization (Vousden, 2000). Since *MDM2* is a direct transcriptional target of p53, there exists a unique autoregulatory feedback loop for inhibiting p53 activity.